First-principles modeling of localized *d* states with the *GW*@LDA+*U* approach

Hong Jiang,[1] Ricardo I. Gomez-Abal,[2] Patrick Rinke,[2] and Matthias Scheffler[2]
[1]*Beijing National Laboratory for Molecular Sciences, National Laboratory of Rare Earth Material Chemistry and Application, Institute of Theoretical and Computational Chemistry, College of Chemistry and Molecular Engineering, Peking University, 100871 Beijing, China*
[2]*Fritz-Haber-Institut der Max-Planck-Gesellschaft, 14195 Berlin, Germany*
(Received 20 April 2010; revised manuscript received 19 June 2010; published 14 July 2010)

First-principles modeling of systems with localized *d* states is currently a great challenge in condensed-matter physics. Density-functional theory in the standard local-density approximation (LDA) proves to be problematic. This can be partly overcome by including local Hubbard *U* corrections (LDA+*U*) but itinerant states are still treated on the LDA level. Many-body perturbation theory in the *GW* approach offers both a quasiparticle perspective (appropriate for itinerant states) and an exact treatment of exchange (appropriate for localized states), and is therefore promising for these systems. LDA+*U* has previously been viewed as an approximate *GW* scheme. We present here a derivation that is simpler and more general, starting from the static Coulomb-hole and screened exchange approximation to the *GW* self-energy. Following our previous work for *f*-electron systems [H. Jiang, R. I. Gomez-Abal, P. Rinke, and M. Scheffler, Phys. Rev. Lett. **102**, 126403 (2009)] we conduct a systematic investigation of the *GW* method based on LDA+*U*(*GW*@LDA+*U*), as implemented in our recently developed all-electron *GW* code FHI-gap (Green's function with augmented plane waves) for a series of prototypical *d*-electron systems: (1) ScN with empty *d* states, (2) ZnS with semicore *d* states, and (3) late transition-metal oxides (MnO, FeO, CoO, and NiO) with partially occupied *d* states. We show that for ZnS and ScN, the *GW* band gaps only weakly depend on *U* but for the other transition-metal oxides the dependence on *U* is as strong as in LDA+*U*. These different trends can be understood in terms of changes in the hybridization and screening. Our work demonstrates that *GW*@LDA+*U* with "physical" values of *U* provides a balanced and accurate description of both localized and itinerant states.

DOI: 10.1103/PhysRevB.82.045108 PACS number(s): 71.10.−w, 71.15.Qe, 71.20.−b

I. INTRODUCTION

Kohn-Sham (KS) density-functional theory (DFT) (Refs. 1 and 2) in the local-density or generalized gradient approximation (LDA/GGA) to the exchange-correlation (xc) energy functional has become "the standard approach" for first-principles electronic-structure calculations of extended systems.[3] Although the Slater-Janak[4,5] transition state theorem relates KS DFT single-particle energies at *half occupation* to excitation energies, KS eigenvalues of a ground-state calculation are often used to interpret excited-state properties as, for example, probed by direct and inverse photoemission spectroscopy (PES/IPES) or optical absorption. This practice, however, should be exercised with caution. Even for weakly correlated systems such as *sp* semiconductors, KS-LDA/GGA band gaps are considerably underestimated (by about 20–50 % compared to experiment).[6] The problem can be more severe for systems with open *d* or *f* shells, often called strongly correlated systems, for which certain wide gap insulators are predicted to be metallic. For these systems, even ground-state properties such as the magnetic ordering might be qualitatively wrong. This is best illustrated in the well-known failure of LDA/GGA for the later transition-metal oxides.[7]

For the quantitative description of quasiparticle excitations in solids as measured by PES/IPES many-body perturbation theory in Hedin's *GW* approximation[8] has become the method of choice. Having earned its merits for *sp* bonded systems, *GW*'s application to *d*- or *f*-electron systems is relatively recent and not as successful as anticipated.[9–30] Applied in the standard way as perturbation to an LDA ground state (G_0W_0@LDA) the *GW* calculation suffers from the pathologies of the LDA starting point.[14–18,20,21,24–26,29,31–35] Following our previous work for *f*-electron systems,[29] we demonstrate in this paper that applying Hubbard *U* corrections to the LDA calculations (LDA+*U*) provides an insightful way to systematically analyze the problem. We investigate examples from three common classes of semiconductors: empty *d* states (ScN), fully filled semicore *d* states (ZnS), and partially filled *d* states (transition-metal oxides NiO, MnO, FeO, and CoO). For physically meaningful values of *U*, G_0W_0 calculations based on LDA+*U* ground states (G_0W_0@LDA+*U*) give a balanced description of both the itinerant and localized states, which is consistent with our previous findings when applying the same approach to *f*-electron systems.[29] Compared to 4*f*-electron systems like lanthanide oxides, where highly localized 4*f* states barely participate in the chemical bonding, typical *d*-electron systems exhibit a much stronger interaction between localized *d* states and itinerant states. It will therefore be elucidating to apply the G_0W_0@LDA+*U* approach to these systems.

The *GW* approximation is the first-order term in a systematic expansion of the self-energy (Σ). The exact Σ could in principle be obtained by solving a set of integrodifferential equations.[8] In practice, this is still beyond the reach of today's computational machinery even for the simplest systems like the homogeneous electron gas. Like this exact set, the *GW* equations could also be solved self-consistently. However, the omission of the vertex function that would introduce higher order interactions with every iteration makes a self-consistent solution inconsistent and worsens the spectral properties of the Green's function.[6,35] In practical calcula-

tions, a "best G best W" strategy is therefore adopted, where the GW quasiparticle energies are expressed as a first-order correction to a reference single-particle Hamiltonian H_0. Both G and W are calculated using eigenenergies and eigenfunctions of H_0, hence the abbreviation G_0W_0.

Early GW studies of late transition-metal oxides, NiO and MnO, showed that G_0W_0 calculations based on LDA single-particle energies and wave functions only slightly improve over the LDA description. However, introducing an approximate level of self-consistency leads to better agreement with experiment.[10,11,13] This indicates that the main difficulty for d/f-electron systems may not come from GW itself, but from the failure of the LDA/GGA as a starting point, although partially occupied d or f states may indeed require the inclusion of higher order correlation effects that go beyond the GW approach. Before venturing into the realm of higher order correlation effects [by, e.g., combining GW with dynamical mean-field theory (DMFT) (Refs. 36 and 37) or through vertex corrections[38,39]] it is important to establish the limitations of the GW approach.

In the spirit of the best G best W approach, much work has been invested recently to develop better single-particle reference Hamiltonians on which to base G_0W_0 quasiparticle energy calculations.[15,21,24–26,32,40–42] In this work we follow the same strategy. For d/f-electron systems, a simple and effective approach to overcome the major failure of LDA/GGA is the LDA+U method in which the LDA total energy is augmented by a local Hubbard correction, characterized by the on-site Coulomb interaction U.[43–46] Since the correction is only applied to a subset of states, LDA+U itself is not expected to provide a quantitatively accurate description of the whole band structure. It can, however, serve as a reasonable starting point for G_0W_0 calculations.[25,29,47] In a previous study,[29] we have applied the G_0W_0@LDA+U approach to f-electron systems, using lanthanide oxides as examples, and found that both localized and itinerant states are described quite accurately and in fact superior to state-of-the-art DMFT. To further assess the performance of the G_0W_0@LDA+U method in a critical manner, we investigate a series of prototypical $3d$-electron systems: (1) ScN with empty d states, (2) ZnS with shallow semicore d states, and (3) transition-metal oxides (MnO, FeO, CoO, and NiO) with partially occupied d states. Although similar conclusion can be reached, $3d$-electron systems also show some significant differences compared to $4f$ systems, and in some sense pose a more serious challenge for first-principles many-body theory calculations.

The paper is organized as follows. In the next section, the main theoretical framework is outlined and certain aspects of our implementation are discussed. In Sec. III, results for three type of representative systems are presented. Section IV summarizes our work.

II. THEORY AND METHODOLOGY

A. *GW* approximation for quasiparticle excitations

Hedin's equations[8] for the Green's function G, the polarizability P, the screened (W) and bare (v) Coulomb interaction, the self-energy Σ, and the vertex function Γ

$$P(1,2) = -i\int G(1,3)G(4,1)\Gamma(3,4,2)d(3,4), \tag{1}$$

$$W(1,2) = v(1,2) + \int v(1,3)P(3,4)W(4,2)d(3,4), \tag{2}$$

$$\Sigma(1,2) = i\int G(1,3)\Gamma(3,4,2)W(4,1)d(3,4), \tag{3}$$

$$\Gamma(1,2,3) = \delta(1,2)\delta(1,3) + \int \frac{\delta\Sigma(1,2)}{\delta G(4,5)} G(4,6)G(7,5)\Gamma(6,7,3)d(4,5,6,7) \tag{4}$$

form a closed set of integrodifferential equations. In Eqs. (1)–(4) we adopted the short-hand form $1 \equiv (\mathbf{r}_1, \sigma_1, t_1)$ to denote a triple of space, spin, and time variables. We will also use $\mathbf{x} = (\mathbf{r}, \sigma)$ to denote the collective space and spin coordinate. Accordingly $\int d(1)$ is a shorthand notation for the integration in all three variables of the triple. By means of Dyson's equation

$$G^{-1}(1,2) = G_0^{-1}(1,2) - \Sigma(1,2), \tag{5}$$

which links the noninteracting system with Green's function G_0 to the fully interacting one (G) via the self-energy Σ, Hedin's equations could, in principle, be solved self-consistently starting from a given G_0.

The GW approximation is formally obtained by retaining only the zeroth-order term in the vertex function $[\Gamma(1,2,3) = \delta(1,2)\delta(1,3)]$. A few attempts to solve this reduced set of equations fully self-consistently have been made in the past.[37,48–59] Although full or partially self-consistent GW calculations can give accurate ground-state total energies and are essential for particle number conservation,[60,61] the quasiparticle properties deteriorate.[49–51] This is a result of the successive introduction of higher order electron-electron interaction terms of certain type that are not balanced by other higher order terms contained in the vertex function.

The most widely used procedure to solve the GW equations in practice is the so-called G_0W_0 approach in which G and W are calculated from the eigenenergies $\{\epsilon_{n\mathbf{k}}\}$ and wave functions $\{\psi_{n\mathbf{k}}\}$ of a single-particle reference Hamiltonian, H_0. The self-energy then takes the form

$$\Sigma(\mathbf{x},\mathbf{x}';\epsilon) = \frac{i}{2\pi}\int d\epsilon' e^{i\epsilon'\eta} G_0(\mathbf{x},\mathbf{x}';\epsilon+\epsilon')W_0(\mathbf{x}',\mathbf{x};\epsilon'), \tag{6}$$

where η is an infinitesimal positive number.[62] The single-particle Green's function G_0 is given by eigenenergies and wave functions of H_0

$$G_0(\mathbf{x},\mathbf{x}';\epsilon) = \sum_{n\mathbf{k}} \frac{\psi_{n\mathbf{k}}(\mathbf{x})\psi_{n\mathbf{k}}^*(\mathbf{x}')}{\epsilon - \tilde{\epsilon}_{n\mathbf{k}}} \tag{7}$$

with $\tilde{\epsilon}_{n\mathbf{k}} \equiv \epsilon_{n\mathbf{k}} + i\eta\,\mathrm{sgn}(\epsilon_F - \epsilon_{n\mathbf{k}})$. W_0 is the screened Coulomb interaction accounting for the weak interaction between the quasiparticles

$$W_0(\mathbf{x},\mathbf{x}';\epsilon) = \int d\mathbf{x}''\epsilon^{-1}(\mathbf{x},\mathbf{x}'';\epsilon)v(\mathbf{x}''-\mathbf{x}'), \tag{8}$$

where $v(\mathbf{x}-\mathbf{x}')=\frac{\delta_{\sigma\sigma'}}{|\mathbf{r}-\mathbf{r}'|}$ is the bare Coulomb interaction and $\epsilon^{-1}(\mathbf{x},\mathbf{x}'';\epsilon)$ the inverse dielectric function. The latter

$$\epsilon(\mathbf{x},\mathbf{x}',\epsilon) = \delta(\mathbf{x}-\mathbf{x}') - \int d\mathbf{x}''v(\mathbf{x}-\mathbf{x}'')P_0(\mathbf{x}'',\mathbf{x}';\epsilon) \tag{9}$$

follows from the polarizability

$$P_0(\mathbf{x},\mathbf{x}';\epsilon) = -\frac{i}{2\pi}\int d\epsilon' e^{\epsilon'\eta}G_0(\mathbf{x},\mathbf{x}';\epsilon+\epsilon')G_0(\mathbf{x}',\mathbf{x};\epsilon'). \tag{10}$$

The QP energies $\mathcal{E}_{n\mathbf{k}}$ are then calculated by first-order perturbation theory, treating $\delta\Sigma \equiv \Sigma - V_{\mathrm{xc}}$ as the perturbation

$$\mathcal{E}_{n\mathbf{k}} = \epsilon_{n\mathbf{k}} + \Re\langle\psi_{n\mathbf{k}}|\Sigma(\mathcal{E}_{n\mathbf{k}}) - V_{\mathrm{xc}}|\psi_{n\mathbf{k}}\rangle, \tag{11}$$

where $V_{\mathrm{xc}}(\mathbf{r})$ is the exchange-correlation potential already included in H_0. Equation (11) is often linearized in energy

$$\begin{aligned}\mathcal{E}_{n\mathbf{k}} &= \epsilon_{n\mathbf{k}} + Z_{n\mathbf{k}}(\epsilon_{n\mathbf{k}})\Re\langle\psi_{n\mathbf{k}}|\Sigma(\epsilon_{n\mathbf{k}}) - V_{\mathrm{xc}}|\psi_{n\mathbf{k}}\rangle \\ &\equiv \epsilon_{n\mathbf{k}} + Z_{n\mathbf{k}}(\epsilon_{n\mathbf{k}})\delta\Sigma_{n\mathbf{k}}(\epsilon_{n\mathbf{k}}),\end{aligned} \tag{12}$$

where the QP renormalization factor $Z_{n\mathbf{k}}$ is given by

$$Z_{n\mathbf{k}}(E) = \left[1 - \left(\frac{\partial}{\partial\epsilon}\Re\langle\psi_{n\mathbf{k}}|\Sigma(\epsilon)|\psi_{n\mathbf{k}}\rangle\right)_{\epsilon=E}\right]^{-1}. \tag{13}$$

For *sp* semiconductors it has been demonstrated that further improvement can be obtained without introducing too much computational overhead by partial self-consistency.[6,63] In the so-called energy-only self-consistent or GW_0 approach the energy denominator in the Green's function is updated by $\mathcal{E}_{n\mathbf{k}}$'s but W remains unchanged.

Recognizing that LDA or GGA are not always the best reference Hamiltonian for a G_0W_0 calculation several alternatives have been proposed.[22,29,32,34,41,42,47,64,65] They roughly fall into two categories. The first comprises different exchange-correlation functionals in H_0, e.g., exact exchange in the optimized effective potential (OEPx) approach,[32,66] hybrid functionals,[34,65] and LDA+U.[25,29,47] All these variants do not increase the computational cost of the G_0W_0 calculation (although some xc functionals might be more computationally expensive than others in the ground-state calculation) but their adequacy is not known *a priori* and has to be carefully investigated on a case by case basis. The second category includes several variants of approximate self-consistency in GW.[15,22,30,41,42,64] These schemes appeal because they remove the dependence of G_0W_0 on the starting point but their nonuniqueness remains a disconcerting factor.

B. LDA+U method

For systems with d/f shells, the severe self-interaction error of LDA or GGA often results in an inadequate description. A simple and effective approach to correct for this is to introduce a local, Hubbard-type correction (LDA+U), characterized by the on-site Coulomb (U) and the exchange interaction (J).[44,46,67] In its most general form, the LDA+U total energy is written as

$$E_{\mathrm{LDA}+U} = E_{\mathrm{LDA}}[\rho^{\sigma}(\mathbf{r})] + E_{\mathrm{ee}}[\hat{n}^{\sigma}] - \bar{E}_{\mathrm{ee}}[n^{\sigma}], \tag{14}$$

where $\sigma=\uparrow,\downarrow$ is the spin index (from now on we will write out the spin degree of freedom explicitly, assuming a collinear spin polarization). $\hat{n}^{\sigma}$ is the local-density matrix defined as

$$n^{\sigma}_{m,m'} = \sum_{n\mathbf{k}} f^{\sigma}_{n\mathbf{k}}\langle m|\psi^{\sigma}_{n\mathbf{k}}\rangle\langle\psi^{\sigma}_{n\mathbf{k}}|m'\rangle, \tag{15}$$

where $f^{\sigma}_{n\mathbf{k}}$ denotes the occupation number of the state $\psi^{\sigma}_{n\mathbf{k}}$ and $\{|m\rangle \equiv |In_plm\rangle\}$ denote a set of atomiclike local orbitals on the Ith atom with the principle, angular, and magnetic quantum numbers n_p, l, and m, respectively. $n^{\sigma} \equiv \mathrm{Tr}\,\hat{n}^{\sigma}$ is the local occupation number. E_{ee} contains the electron-electron interaction of the localized electrons and the double-counting term $\bar{E}_{\mathrm{ee}}$ removes the part that was already included in the LDA Hamiltonian. The LDA+U approach is obtained by treating E_{ee} in a Hartree-Fock-type fashion[45]

$$\begin{aligned}E_{\mathrm{ee}}[\hat{n}^{\sigma}] = \frac{1}{2}\sum_{\{m=-l,l\},\sigma} \{&(\langle m_1,m_2|V_{\mathrm{ee}}|m_3,m_4\rangle \\ &- \langle m_1,m_2|V_{\mathrm{ee}}|m_4,m_3\rangle)n^{\sigma}_{m_3m_1}n^{\sigma}_{m_4m_2} \\ &+ \langle m_1,m_2|V_{\mathrm{ee}}|m_3,m_4\rangle n^{\sigma}_{m_3m_1}n^{-\sigma}_{m_4m_2}\}\end{aligned} \tag{16}$$

with an effective screened Coulomb interaction V_{ee}. Using the angular expansion of V_{ee}

$$V_{\mathrm{ee}}(\mathbf{r},\mathbf{r}') = \sum_{L}\sum_{M=-L}^{L} v_L(r,r')\frac{4\pi}{2L+1}Y_{LM}(\hat{\mathbf{r}})Y^*_{LM}(\hat{\mathbf{r}}'), \tag{17}$$

the Coulomb matrix element $\langle m_1,m_2|V_{\mathrm{ee}}|m_3,m_4\rangle$ can be expanded as follows:

$$\langle m_1,m_2|V_{\mathrm{ee}}|m_3,m_4\rangle = \sum_{L} F_L C_L(m_1,m_2,m_3,m_4). \tag{18}$$

F_L are radial Coulomb integrals (Slater's integrals)

$$F_L \equiv \int dr\int dr' r^2r'^2|R_{n_pl}(r)|^2 v_L(r,r')|R_{n_pl}(r')|^2 \tag{19}$$

and $C_L(m_1,m_2,m_3,m_4)$ are angular integrals, which, using Wigner's three-j symbols,[68] read

$$\begin{aligned}C_L(m_1,m_2,m_3,m_4) = \sum_{M=-L}^{L} &(2l+1)^2(-1)^{m_1+m_2+M} \\ &\times \begin{pmatrix} l & L & l \\ 0 & 0 & 0\end{pmatrix}^2 \begin{pmatrix} l & L & l \\ -m_1 & -M & m_3\end{pmatrix} \\ &\times \begin{pmatrix} l & L & l \\ -m_2 & M & m_4\end{pmatrix}.\end{aligned} \tag{20}$$

For d electrons, only F_0, F_2, and F_4 are nonvanishing, and they are related to U and J by $U=F_0$ and $J=(F_2+F_4)/14$. By fixing the ratio F_4/F_2, which is nearly constant ($\sim$0.625) in

free atoms,[69] one can use U and J as only parameters to determine E_{ee}.[45,46]

The double-counting correction term $\bar{E}_{ee}[n^\sigma]$, on the other hand, is more arbitrary and is one of the largest problems in the LDA+U approach.[44,45,67,70–73] Most frequently $\bar{E}_{ee}$ is taken as the following function of the local occupation numbers n^σ:

$$\bar{E}_{ee}[n^\sigma] = \frac{1}{2}Un(n-1) - \frac{1}{2}J\sum_\sigma n^\sigma(n^\sigma - 1), \tag{21}$$

which can be obtained from Eq. (16) by neglecting orbital polarization effects, often called fully localized limit (FLL).[70,74]

The single-particle Hamiltonian corresponding to $E_{LDA+U}[\rho(\mathbf{r})]$ reads

$$H_0^{LDA+U,\sigma} = -\frac{1}{2}\nabla^2 + V_{ext} + V_H + V_{xc}^\sigma + \delta\hat{V}^\sigma, \tag{22}$$

where $\delta\hat{V}^\sigma \equiv \Sigma_{mm'}|m\rangle\delta V_{mm'}^\sigma\langle m'|$ is a site- and orbital-dependent nonlocal potential arising from the LDA+U correction term,

$$\begin{aligned}\delta V_{mm'}^\sigma &\equiv \frac{\delta\{E_{ee}[\hat{n}^\sigma] - \bar{E}_{ee}[n^\sigma]\}}{\delta n_{mm'}^\sigma} \\ &= \sum_{m_1m_2}\langle mm_1|V_{ee}|m'm_2\rangle n_{m_2,m_1} - \langle mm_1|V_{ee}|m_2m'\rangle n_{m_2,m_1}^\sigma \\ &\quad - \delta_{mm'}\left[\left(n-\frac{1}{2}\right)U - \left(n^\sigma - \frac{1}{2}\right)J\right].\end{aligned} \tag{23}$$

Neglecting the anisotropy of the local Coulomb interaction, i.e., dropping all $L>0$ terms in Eq. (17) and further using the identity $C_{L=0}(m_1,m_2,m_3,m_4) = \delta_{m_1,m_3}\delta_{m_2,m_4}$,[68] we obtain

$$\langle m_1,m_2|V_{ee}|m_3,m_4\rangle \simeq F_0\delta_{m_1m_3}\delta_{m_2m_4}. \tag{24}$$

Within this approximation we have

$$\delta V_{mm'}^\sigma = \left[\frac{1}{2}\delta_{mm'} - n_{mm'}^\sigma\right]U. \tag{25}$$

If we define the local projection so that the on-site density matrix is diagonal, $\delta\hat{V}$ takes the simple form

$$\delta\hat{V}^\sigma = \sum_m U\left(\frac{1}{2} - n_m^\sigma\right)|m\rangle\langle m|. \tag{26}$$

The main physical effect of $\delta\hat{V}$ is therefore to push occupied localized states down and unoccupied ones up in energy, which effectively opens a gap that might have been absent in the LDA description.

C. LDA+U as an approximation to GW

For *highly localized* d/f states LDA+U can be viewed as an approximate GW scheme, as first pointed out by Anisimov *et al.*[46] The original derivation is fairly involved and based on several specific assumptions that turn out to be not necessary. We present here a derivation that is simpler and more general, starting from the static Coulomb-hole and screened exchange (COHSEX) approximation[6,8] to the GW self-energy. The COHSEX approximation is obtained by omitting the dynamic features of the screened Coulomb interaction

$$\begin{aligned}\Sigma^\sigma(\mathbf{r},\mathbf{r}') &\simeq \frac{1}{2}\delta(\mathbf{r}-\mathbf{r}')[W(\mathbf{r},\mathbf{r}';0) - v(\mathbf{r}-\mathbf{r}')] \\ &\quad - \sum_{n\mathbf{k}} f_{n\mathbf{k}}^\sigma\psi_{n\mathbf{k}}^\sigma(\mathbf{r})\psi_{n\mathbf{k}}^{\sigma*}(\mathbf{r}')W(\mathbf{r},\mathbf{r}';0).\end{aligned} \tag{27}$$

Using the closure relation of the KS states

$$\delta(\mathbf{r},\mathbf{r}') = \sum_{n\mathbf{k}}\psi_{n\mathbf{k}}^\sigma(\mathbf{r})\psi_{n\mathbf{k}}^{\sigma*}(\mathbf{r}'), \tag{28}$$

we obtain

$$\begin{aligned}\Sigma^\sigma(\mathbf{r},\mathbf{r}') &= \sum_{n\mathbf{k}}\left(\frac{1}{2} - f_{n\mathbf{k}}^\sigma\right)\psi_{n\mathbf{k}}^\sigma(\mathbf{r})\psi_{n\mathbf{k}}^{\sigma*}(\mathbf{r}')W(\mathbf{r},\mathbf{r}';0) \\ &\quad - \frac{1}{2}\sum_{n\mathbf{k}}\psi_{n\mathbf{k}}^\sigma(\mathbf{r})\psi_{n\mathbf{k}}^{\sigma*}(\mathbf{r}')v(\mathbf{r},\mathbf{r}').\end{aligned} \tag{29}$$

The matrix elements of $\Sigma^\sigma(\mathbf{r},\mathbf{r}')$ projected onto the local subspace $\{|m\rangle\}$ can therefore be written as

$$\begin{aligned}\Sigma_{mm'}^\sigma &= \sum_{n\mathbf{k}}\left(\frac{1}{2} - f_{n\mathbf{k}}^\sigma\right)\langle\phi_m\psi_{n\mathbf{k}}^\sigma|W(0)|\psi_{n\mathbf{k}}^\sigma\phi_{m'}\rangle \\ &\quad - \frac{1}{2}\sum_{n\mathbf{k}}\langle\phi_m\psi_{n\mathbf{k}}^\sigma|v|\psi_{n\mathbf{k}}^\sigma\phi_{m'}\rangle.\end{aligned} \tag{30}$$

We now decompose the Kohn-Sham wave functions according to

$$|\psi_{n\mathbf{k}}^\sigma\rangle = \sum_m C_{m;n\mathbf{k}}^\sigma|\phi_m\rangle + |\tilde{\psi}_{n\mathbf{k}}^\sigma\rangle \tag{31}$$

with $C_{m;n\mathbf{k}}^\sigma \equiv \langle\phi_m|\psi_{n\mathbf{k}}^\sigma\rangle$. $|\tilde{\psi}_{n\mathbf{k}}^\sigma\rangle$ can be regarded as a "pure" itinerant state in which the contribution of localized states has been projected out. Inserting Eq. (31) into Eq. (30) and further assuming that *any matrix element that involves the overlap of* $\phi_m(\mathbf{r})$ and $\tilde{\psi}_{n\mathbf{k}}(\mathbf{r})$ can be neglected, we obtain

$$\begin{aligned}\Sigma_{mm'}^\sigma &= \sum_{m_1m_2}\sum_{n\mathbf{k}}\left\{\left(\frac{1}{2} - f_{n\mathbf{k}}^\sigma\right)C_{m_1;n\mathbf{k}}^{\sigma*}C_{m_2;n\mathbf{k}}^\sigma\right. \\ &\quad \left.\times\langle mm_1|W(0)|m_2m'\rangle - \frac{1}{2}C_{m_1;n\mathbf{k}}^{\sigma*}C_{m_2;n\mathbf{k}}^\sigma\langle mm_1|v|m_2m'\rangle\right\} \\ &= \sum_{m_1m_2}\left(\frac{1}{2}\delta_{m_1m_2} - n_{m_2m_1}^\sigma\right)\langle mm_1|W(0)|m_2m'\rangle \\ &\quad - \frac{1}{2}\sum_{m_1}\langle mm_1|v|m_1m'\rangle,\end{aligned} \tag{32}$$

where we have used the relations

$$\sum_{n\mathbf{k}} f_{n\mathbf{k}}^\sigma C_{m_1;n\mathbf{k}}^{\sigma*}C_{m_2;n\mathbf{k}}^\sigma \equiv n_{m_2m_1}^\sigma,$$

$$\sum_{n\mathbf{k}} C^{\sigma *}_{m_1;n\mathbf{k}} C^{\sigma}_{m_2;n\mathbf{k}} \equiv \delta_{m_1 m_2}. \tag{33}$$

In the spirit of the LDA+U approach, we consider only corrections to localized states

$$\delta V^{\sigma}_{mm'} = \langle m | V^{\mathrm{loc}}_{\mathrm{H}} + \Sigma^{\sigma} - V^{\mathrm{loc},\sigma}_{\mathrm{LDA}} | m' \rangle, \tag{34}$$

where $V^{\mathrm{loc}}_{\mathrm{H}}$ is the Hartree potential of the localized electron density

$$n^{\mathrm{loc}}(\mathbf{r}) \equiv \sum_{m_1 m_2} n_{m_1 m_2} \phi_{m_1}(\mathbf{r}) \phi^{*}_{m_2}(\mathbf{r}), \tag{35}$$

$$[V^{\mathrm{loc}}_{\mathrm{H}}]_{mm'} \equiv \langle m | V^{\mathrm{loc}}_{\mathrm{H}} | m' \rangle = \sum_{m_1 m_2} n_{m_2 m_1} \langle m m_1 | v | m' m_2 \rangle. \tag{36}$$

$V^{\mathrm{loc},\sigma}_{\mathrm{LDA}}(\mathbf{r}) \equiv \delta \bar{E}^{\mathrm{loc}}_{\mathrm{ee}} / \delta \rho^{\sigma}(\mathbf{r})$ is the interaction potential among the localized states in the LDA. Using a similar argument as for the FLL approximation to the double-counting correction, i.e. Eq. (21), we obtain

$$\bar{E}^{\mathrm{loc}}_{\mathrm{ee}} = \frac{1}{2} F^{(0)}_0 n(n-1) - \frac{1}{2} J^{(0)} \sum_{\sigma} n^{\sigma}(n^{\sigma} - 1),$$

$$V^{\mathrm{loc},\sigma}_{\mathrm{LDA}}(\mathbf{r}) = \left(n - \frac{1}{2}\right) F^{(0)}_0 - \left(n^{\sigma} - \frac{1}{2}\right) J^{(0)}, \tag{37}$$

where $F^{(0)}_0$ and $J^{(0)}$ are the first Slater integral and the on-site exchange term from the bare Coulomb interaction $v(\mathbf{r},\mathbf{r}')$, respectively.

We therefore have

$$\delta V^{\sigma}_{mm'} = \sum_{m_1 m_2} \left\{ n_{m_2 m_1} \langle m m_1 | v | m' m_2 \rangle + \left(\frac{1}{2} \delta_{m_1 m_2} - n^{\sigma}_{m_2 m_1} \right) \times \langle m m_1 | W(0) | m_2 m' \rangle \right\} - \frac{1}{2} \sum_{m_1} \langle m m_1 | v | m_1 m' \rangle - \delta_{mm'} \left[\left(n - \frac{1}{2} \right) F^{(0)}_0 - \left(n^{\sigma} - \frac{1}{2} \right) J^{(0)} \right]. \tag{38}$$

By neglecting the anisotropy in both the bare and screened Coulomb interaction, i.e., using the approximation in Eq. (24), we obtain exactly the same expression as in LDA+U [Eq. (25)]

$$\delta V^{\sigma}_{mm'} = \left[\frac{1}{2} \delta_{mm'} - n^{\sigma}_{mm'} \right] U, \tag{39}$$

where U is identified as the first Slater integral F_0 arising from the static screened Coulomb interaction $W(\mathbf{r},\mathbf{r}';0)$.[46]

To summarize, LDA+U follows from the GW approach under the assumption that: (1) The frequency dependence of the screened Coulomb interaction is neglected; (2) quasiparticle corrections are only applied to localized states, whereas itinerant states are still treated at the LDA level; (3) all Coulomb matrix elements that involve the overlap of a localized state and an itinerant state are neglected (which is equivalent to omitting the many-body exchange interaction between localized and itinerant electrons).

None of these assumptions are of course fully satisfied in realistic systems. The dynamic character of the screened Coulomb interaction is actually stronger for localized electrons than for itinerant ones, as demonstrated by the fact that the renormalization factor [Eq. (13)] typically takes a value of ~0.5–0.6 for localized states, in contrast to the typical value of ~0.8–0.9 for itinerant states.[24] The LDA description of the itinerant states suffers from the band-gap problem and the coupling between localized and itinerant states is critical for the physical and chemical properties of d/f-electron systems.

D. GW@LDA+U method

The preceding discussion elucidates that LDA+U is a relatively crude approximation to GW and is therefore not necessarily expected to provide an accurate description of d or f-electron systems on its own. However, since LDA+U corrects the major failure of LDA for localized systems, it is likely to serve as a good starting point for G_0W_0 and GW_0 (i.e. energy-only self-consistent GW with fixed W_0) calculations. Formally, the only difference between the LDA- and LDA+U-based GW formalism is the contribution of $\delta\hat{V}$

$$\mathcal{E}^{\sigma}_{n\mathbf{k}} = \epsilon^{\sigma}_{n\mathbf{k}} + \Re[\langle \psi^{\sigma}_{n\mathbf{k}} | \Sigma(\mathcal{E}^{\sigma}_{n\mathbf{k}}) - V^{\sigma}_{\mathrm{xc}} - \delta\hat{V}^{\sigma} | \psi^{\sigma}_{n\mathbf{k}} \rangle]. \tag{40}$$

This equation illustrates that the double-counting term contained in $\epsilon_{n\mathbf{k}}$ is exactly canceled out in the GW@LDA+U approach, which is a significant advantage of the scheme.

Before we introduce the specific values of U for the systems in this work, we will treat U as a parameter and analyze the U dependence of GW@LDA+U, which is quite different from that of LDA+U. The $\delta\hat{V}$ contribution in the LDA+U single-particle energies can be split off

$$\epsilon^{\sigma}_{n\mathbf{k}} = \langle \psi^{\sigma}_{n\mathbf{k}} | -\frac{1}{2}\nabla^2 + V^{\sigma}_{\mathrm{LDA}} + \delta\hat{V}^{\sigma} | \psi^{\sigma}_{n\mathbf{k}} \rangle = \bar{\epsilon}^{\sigma}_{n\mathbf{k}} + \delta\hat{V}^{\sigma}_{n\mathbf{k}} \tag{41}$$

and $\bar{\epsilon}^{\sigma}_{n\mathbf{k}}$ can be regarded as LDA single-particle energies calculated with LDA+U wave functions. If we now expand the self-energy around $\bar{\epsilon}^{\sigma}_{n\mathbf{k}}$ instead of $\epsilon^{\sigma}_{n\mathbf{k}}$, under the assumption that $\Sigma^{\sigma}_{n\mathbf{k}}(E)$ can be approximated by a linear function around $\epsilon^{\sigma}_{n\mathbf{k}}$ we obtain, after some simple algebraic manipulations,

$$\mathcal{E}^{\sigma}_{n\mathbf{k}} = \bar{\epsilon}^{\sigma}_{n\mathbf{k}} + Z_{n\mathbf{k}}(\bar{\epsilon}^{\sigma}_{n\mathbf{k}}) [\Sigma^{\sigma}_{n\mathbf{k}}(\bar{\epsilon}^{\sigma}_{n\mathbf{k}}) - (V_{\mathrm{xc}})^{\sigma}_{n\mathbf{k}}]. \tag{42}$$

Equation (42) has no explicit U dependence and the quasiparticle energies in GW@LDA+U therefore depend only implicitly on U. The two main factors are (1) the difference in wave functions between LDA+U and LDA, and (2) the change in screening introduced by changes in the single-particle spectrum, most notably the band gap. Regarding point (1), occupied states with strong d/f character will be pushed toward lower energies and become more localized, whereas unoccupied states with strong d/f character are pushed to higher energies and become more delocalized. This implies that $\bar{\epsilon}^{\sigma}_{n\mathbf{k}}$ in Eq. (42) is larger for more localized states. The U dependence of the second term in Eq. (42) is

determined by the change in screening, which can be characterized by the macroscopic static dielectric constant,

$$\epsilon_M \equiv [\lim_{\mathbf{q}\to 0} \epsilon^{-1}(\mathbf{q},\mathbf{q},\omega=0)]^{-1}. \quad (43)$$

Increasing U usually increases the band gap and therefore reduces ϵ_M. The limit of vanishing screening gives the Hartree-Fock self-energy, whose corresponding band gap is dramatically overestimated. The second term therefore has a tendency to increase the $GW@\mathrm{LDA}+U$ band gap with increasing U. In practice both terms can significantly shape the U dependence of the system under study, as we will demonstrate in the next section.

E. Computational details

All DFT calculations are performed using the WIEN2K package[75] in which the Kohn-Sham equations are solved in the full-potential (linearized) augmented plane wave plus local orbital [FP−(L)APW+lo] approach.[76] The following parameters for the FP−(L)APW+lo basis are used: muffin-tin (MT) radii R_{MT} (in units of Bohr) are (2.13, 1.89) for ScN, (2.05, 1.95) for ZnS, (2.10, 1.86) for MnO, (2.10, 1.77) for FeO, (2.05, 1.75) for CoO, and (1.97, 1.75) for NiO; wave functions are expanded by spherical harmonics with l up to $l_{\max}=10$ in the MT spheres, and by plane waves with the energy cutoff determined by min $R_{\mathrm{MT}}\times K_{\max}=7.0$ in the interstitial (IS) region; the potential and electron density are expanded in cubic harmonics l up to $l_{\max}=4$ within the MT spheres, and by plane waves in the IS region. For the LDA+U calculations, the double-counting correction is treated in the FLL scheme [i.e., Eq. (21), LDA+U, self-interaction correction (SIC) in the WIEN2K notation].[44,77] GW calculations were performed using the FHI-gap (Green's function with augmented plane waves) package, a recently developed all-electron GW add on to WIEN2K.[29,78–80] All important convergence parameters have been monitored to achieve an overall numerical accuracy of ≃0.05 eV. The Brillioun zone was sampled with $4\times4\times4$ **k** meshes; unoccupied states with energy up to 136 eV were taken into account. Densities of states (DOSs) are calculated using ~1000 **k** points in the Brillouin zone. In the GW case, DOS are obtained from GW quasiparticle energies, first calculated on the sparse **k** mesh and then interpolated to the fine **k** mesh (~1000) using the Fourier interpolation technique.[81] When the calculated DOS is compared to the experimental spectral data, a Gaussian broadening of 0.6 eV was chosen to mimic typical experimental resolutions.

We use the experimental lattice constants for all materials considered in the next section. ScN has a NaCl structure with $a(\mathrm{exp})=4.50$ Å.[82] ZnS takes the zinc-blende structure with $a(\mathrm{exp})=5.42$ Å taken from Ref. 63. The transition-metal monoxides (MO, M=Mn, Fe, Co, and Ni) crystallize in the NaCl structure in the paramagnetic phase. In this work, however, we consider the type-II antiferromagnetic (AFM-II) phase, which is the most stable structure below the Neel temperature.[7] Experimental lattice constants for MnO, FeO, CoO, and NiO are taken from Ref. 83: $a=4.445$ Å, 4.334 Å, 4.254 Å, and 4.171 Å, respectively.

III. $GW@\mathrm{LDA}+U$ FOR LOCALIZED d STATES

A. Determination of U

The parameters U and J describe the effective Coulomb and exchange interaction between localized electrons in a crystalline environment. The determination of U from first principles has attracted growing interest in recent years.[67,74,84–92] The most widely used approach is the constrained DFT formalism, which was developed in a general form by Dederichs *et al.*[86] and later widely used to calculate parameters for effective Hamiltonians (Hubbard or Anderson).[93,94] The Hubbard U is obtained from the total-energy variation for different integer occupations of a fictitious atom (usually denoted the impurity) embedded in a crystalline environment via the supercell technique. In practice, a constrained DFT calculation proceeds along the following lines (using NiO as an example): (1) in a supercell of NiO one Ni atom is treated as an "impurity;" (2) a suitable constraint (see below) is imposed that allows variations in the local occupation number of the impurity $3d$ states (n_d) while keeping the system as a whole neutral (by either changing the number of valence electrons correspondingly or adding a uniform compensating charge); (3) from the corresponding total energy $E(n_d^\uparrow,n_d^\downarrow)$ for different occupations U and J are determined according to

$$U-J=E(n_d^\uparrow+1,n_d^\downarrow)+E(n_d^\uparrow-1,n_d^\downarrow)-2E(n_d^\uparrow,n_d^\downarrow), \quad (44)$$

$$J=\frac{1}{m_d+1}[E(n_d^\uparrow,n_d^\downarrow)-E(n_d^\uparrow+1,n_d^\downarrow-1)] \quad (45)$$

with $m_d\equiv n_d^\uparrow-n_d^\downarrow$. There are different ways to constrain n_d, depending on the definition of the local projection and the implementation for the Kohn-Sham equations. In Anisimov and Gunnarsson's original work,[67] the $3d$ electrons were constrained by setting the hopping integrals between the impurity $3d$ orbitals and other orbitals to zero in their linear muffin-tin orbital (LMTO) code based on the atomic sphere approximation (ASA). In the linearized augmented plane wave (LAPW) framework as implemented in WIEN2K, the constraint is imposed by removing the d orbitals on the impurity from the LAPW basis and treating the impurity $3d$ states as core states with fixed occupation number.[95] Alternatively one can also constrain n_d to the desired value by solving a constrained optimization problem[84,91]

$$E(n_d^\sigma)\equiv \min_{\rho^\sigma(\mathbf{r});\mathrm{Tr}\,\hat{n}^\sigma=n_d} E_{\mathrm{LDA}}[\rho^\sigma(\mathbf{r})]. \quad (46)$$

This approach is more general and applicable to any code as long as the local projection in Eq. (15) can be defined. The values of U obtained from constrained DFT can depend significantly on the implementation of the constraint and are additionally basis set specific. This explains the spread of U's reported in the literature for the same material by different groups. However, as long as a consistent approach is adopted at all stages, i.e., the same basis set and local projectors are used in the constrained DFT and subsequent LDA+U and $G_0W_0@\mathrm{LDA}+U$ calculations, as in our work, the U values are meaningful.

TABLE I. Hubbard parameters U and J (in units of eV) obtained from constrained DFT calculations for the materials investigated in this work. Other theoretically determined U values reported in the literature are also collected for comparison.

Materials	ScN	ZnS	MnO	FeO	CoO	NiO
U	3.6	7.1	4.7	4.8	5.1	5.2
J	0.7	1.1	0.8	0.9	0.9	0.9
Other reported U values						
Anisimov *et al.*[a]			6.9	6.8	7.8	8.0
Pickett *et al.*[b]			3.6	4.6	5.0	5.1
Cococcioni and de Geroncoli[c]				4.3		4.6

[a]Reference 43.
[b]Reference 84.
[c]Reference 85.

For transition-metal oxides, the U's obtained in the LMTO-ASA based constrained DFT calculations by Anisimov, Zaanen, and Andersen (AZA) (Ref. 43) have been widely applied.[83] However, several reports in the literature indicate that these U's are too large.[71,96,97] More recent studies employing the linear-response approach[84,85] or the constrained random-phase approximation (RPA) (Refs. 90 and 98) yield significantly smaller U's. In this work, U's and J's were calculated with constrained DFT as implemented in the LAPW basis.[95] Our values of U are listed in Table I. They are significantly smaller than AZA's but very close to the linear response and constrained RPA ones.[84,85,92] The difference between our and AZA's constrained DFT results can be attributed to the different basis used in the calculations, i.e., full-potential vs atomic sphere approximation, and LAPW vs LMTO.

In practical LDA+U calculations, U and J are often combined by redefining U as $U_{\text{eff}}=U-J$ and setting $J=0$.[71] We found that such a simplification can have noticeable effects on the resultant electronic properties, as also recently reported by Ylvisaker and Pickett.[73] We therefore only use $J=0$ when investigating the U dependence but use the finite J's as obtained by Eq. (45) and listed in Table I when we compare our G_0W_0@LDA+U results to experiment.

B. ScN: Empty *d* states

The 3*d* states in ScN form the lowest conduction bands and apart from a small hybridization with the valence bands are nearly empty.[99,100] Interest in ScN has recently increased both experimentally and theoretically due to its possible application in optoelectronic devices.[100–104] LDA predicts ScN to be a semimetal with a negative band gap of −0.14 eV. Recent calculations based on the exact-exchange OEPx (Ref. 101) or the screened exchange approach[99] predict a semiconductor with an indirect Γ-X band gap with the respective Kohn-Sham band gaps of 1.7 and 1.6 eV. G_0W_0 calculations based on OEPx, on the other hand, give an indirect band gap of 0.84 eV.[100] Based on optical-absorption spectroscopy and ultraviolet valence-band photoemission, Gall *et al.* obtained

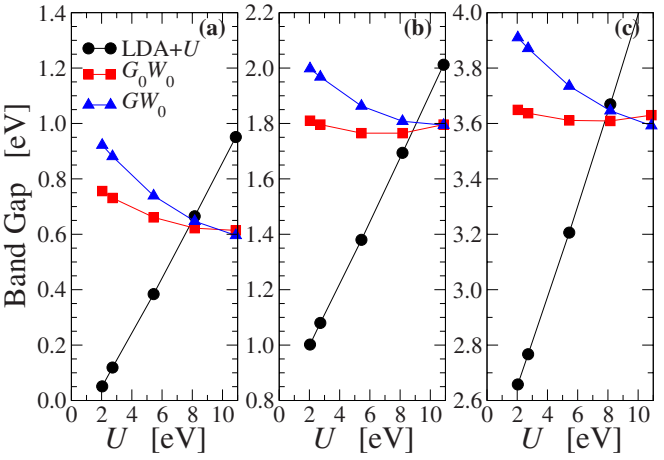

FIG. 1. (Color online) Band gaps of ScN as a function of U ($J=0$) calculated by LDA+U (circles) and G_0W_0/GW_0@LDA+U (squares): (a) $E_g^{\Gamma\text{-X}}$, (b) $E_g^{\text{X-X}}$, and (c) $E_g^{\Gamma\text{-}\Gamma}$.

an indirect gap of 1.3 ± 0.3, where the sizable error bar of 0.3 eV was mainly attributed to the presence of conduction electrons in the ScN thin films used in the measurement. This value was later revised by the same authors in a more careful experimental study with significantly reduced free-electron concentrations; the combination of scanning tunneling spectroscopy and optical absorption gives an indirect gap of 0.9 ± 0.1 eV and a direct gap of 2.15 eV.[103]

Figure 1 shows the indirect ($E_g^{\Gamma\text{-X}}$) and direct ($E_g^{\text{X-X}}$ and $E_g^{\Gamma\text{-}\Gamma}$) band gaps of ScN in LDA+U, G_0W_0, and GW_0@LDA+U as a function of U. In LDA+U, ScN becomes insulating when U is larger than ~2.0 eV and the gap increases almost linearly with increasing U. To obtain the experimental band gap of about 0.9 eV, the Hubbard U would have to be as large as 10 eV, much larger than the $U-J=2.9$ eV obtained from constrained DFT calculations and clearly unphysical. Conversely, in G_0W_0 and GW_0@LDA+U the band gaps decrease with increasing U. With the exception of very large $U(>\sim9$ eV) the GW_0 band gaps are always larger than G_0W_0 ones, similar to what is usually observed for *sp* semiconductors.[63]

This somewhat peculiar U dependence of GW@LDA+U can be understood by analyzing the effects of U on the single-particle energies and wave functions from LDA+U using Eq. (42), which is shown for the direct gap at the Γ point in Fig. 2. To cross-check that Eq. (42) is valid in this case we have verified that it gives nearly the same band gaps as Eq. (40) (circles and crosses in the right panel of Fig. 2). With increasing U, the two terms in Eq. (42) exhibit the opposite behavior. $\bar{\epsilon}_{n\mathbf{k}}^{\text{LDA}}$, the LDA single-particle energies calculated with LDA+U wave functions, decreases, because the bottom of the conduction, which is mainly of Sc 3*d* character, is pushed upward strongly by the U-dependent correction term and becomes more delocalized, whereas the N 2*p* character leaves the top of the valence band largely independent of U. Conversely, the second term increases, because a larger LDA+U band-gap results in weaker screening, as demonstrated by the decreasing dielectric constant (right panel of Fig. 2). As a result, the self-energy in the second term of Eq. (42) increases the band gap with increasing U.

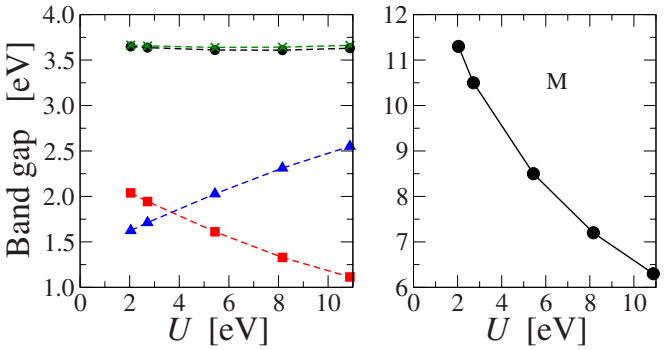

FIG. 2. (Color online) Analysis of the U dependence for the band gap of ScN. Left panel: the direct band gap at $\mathbf{k}=0$ obtained from Eq. (40) (circles), from Eq. (42) (crosses), and the contributions from the first (squares) and second (triangles) term in Eq. (42) as a function of U; Right panel: the static macroscopic dielectric function calculated by LDA+U orbital energies and wave functions as a function of U.

We note that the U dependence in ScN is similar to that of the empty $4f$-shell compound CeO_2.[29] The band gap in CeO_2 is formed between valence-band states of predominantly oxygen $2p$ character and unoccupied $4f$ states that lie below conduction-band states of predominantly $5d$ character. The p-f gap depends strongly on U in LDA+U but is nearly constant in G_0W_0@LDA+U.[29]

In Table II different theoretical band gaps of ScN are compared to experiment. The G_0W_0@LDA band gaps were obtained by extrapolating the G_0W_0@LDA+U results to the $U-J\rightarrow 0$ limit via a quadratic fitting function. We verified that this gives nearly the same band gaps (0.94 vs 0.87 eV) as extrapolating the G_0W_0@LDA band gaps for different lattice constants, following the same procedure as in Ref. 100. We further note that the G_0W_0@LDA band gaps for ScN in this work differ from those in Ref. 100, where a pseudopotential plane-wave implementation was used. The discrepancy of ~0.2 eV is likely due to the core-valence exchange-correlation partitioning and pseudoization error of the pseudopotential GW approach.[78] In general our GW results are in good agreement with experiment, whereby the best agreement is achieved by GW_0@LDA+U.

C. ZnS: Semicore *d* states

It has been recognized that the G_0W_0@LDA approach performs worse for systems with shallow semicore d states, e.g., II_B-VI compounds or group-III nitrides, than for other sp semiconductors. The actual reason is still a matter of debate but it is likely that it is associated to the absence of strong short-range correlations in the GW approximation.[35,42,63,105–110] The error in the band gap can be considerable and the binding energies of semicore d electrons (ϵ_d) are significantly underestimated. Miyake *et al.*[47] have recently studied ZnS in G_0W_0@LDA+U with a particular emphasis on the d-band position. They found that (1) using $U=8$ eV and $J=1$ eV, LDA+U reproduces the experimental d-band position but the band gap is still significantly underestimated; (2) G_0W_0@LDA+U pushes the d bands back to their G_0W_0@LDA values. The same observation was made by Shishkin and Kresse.[63] In a more recent study by the same authors[42] it was shown that partial self-consistency in GW improves the description of band gaps for II_B-VI compounds but the error in ϵ_d remains large even when both self-consistency and an improved dielectric function in W are taken into account.[42] It was further argued that a more accurate description for the d-electron binding energies will require vertex corrections in both W and the self-energy.

TABLE II. Indirect and direct band gaps (in eV) of ScN obtained with different approaches. $U=3.6$ eV and $J=0.7$ eV are used in LDA+U and GW@LDA+U calculations.

Approach	$E_g^{\Gamma\text{-}X}$	$E_g^{X\text{-}X}$	$E_g^{\Gamma\text{-}\Gamma}$
LDA	−0.14	0.78	2.34
G_0W_0@LDA	0.87	1.92	3.69
GW_0@LDA	1.07	2.11	4.05
LDA+U	0.16	1.13	2.84
G_0W_0@LDA+U	0.75	1.84	3.63
GW_0@LDA+U	0.85	1.95	3.85
G_0W_0@LDA [a]	1.14	2.06	3.71
G_0W_0@OEPx(cLDA) [a]	0.84	1.98	3.51
Expt.[b]	1.30 ± 0.3	2.40	~3.8
Expt.[c]	0.9 ± 0.1	2.15	

[a]Reference 100.
[b]Reference 101.
[c]Reference 103.

Our own LDA+U based G_0W_0 and GW_0 calculations for ZnS are summarized in Fig. 3 and confirm these observations. Since the semicore d states are fully occupied and fall between the S $2p$ and S $2s$ derived bands, the effect of U on the band gap is indirect and very weak. The valence and conduction bands change only slightly for U's from 0 to 11 eV, and the band gap increases by 0.42 eV, 0.28 eV, and 0.24 eV in LDA+U, G_0W_0, and GW_0, respectively. This is consistent with the fact that the orbital-dependent potential $\delta\hat{V}$ is applied only to the d states and influences the band gap mainly through the p-d coupling.[111] With increasing $U-J$, ϵ_d increases linearly in LDA+U and reaches the experimental value at $U\sim10$ eV, which is considerably higher than our $U-J$ value of ~6.0 eV obtained from constrained DFT. In addition, once the GW corrections are added to the LDA+U energies, the G_0W_0 and GW_0 results become very similar to the respective LDA-based GW calculations and exhibit only a very weak variation with U. The inset of Fig. 3 shows the RPA dielectric constant ϵ_M, which decreases as U increases. But even at U as large as 10.9 eV, ϵ_M is still significantly overestimated when compared to experiment, which is consistent with the underestimation of the band gap in G_0W_0 and GW_0.

D. Transition-metal monoxides

The transition-metal monoxides MnO, FeO, CoO, and NiO are frequently considered to be prototypical strongly

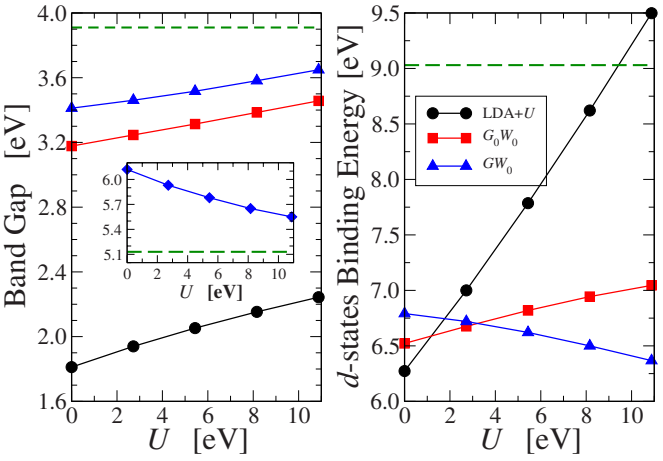

FIG. 3. (Color online) Band gap (left) and average *d*-electron binding energy (right) of ZnS calculated with LDA+U (circles), G_0W_0 (squares), and GW_0 (triangles) as a function of U (J=0). Dashed lines are the corresponding experimental values taken from Ref. 63. The inset in the left panel shows the macroscopic dielectric constant calculated from the LDA+U energies and wave functions.

correlated electron systems and have become testbeds for many new first-principles approaches.[10,15,21,25,43,83,96,112–116] The four compounds roughly fall into two classes: (1) MnO and NiO, for which standard band theory within LDA or GGA still predicts an insulating ground state when applied in the AFM-II phase but with significantly underestimated band gaps; (2) FeO and CoO, for which LDA and GGA give metallic ground states even in the AFM-II phase.[7] In this work we consider only the AFM-II phase. Further investigations concerning the relation between magnetic ordering and electronic band structures will be reported elsewhere.

1. MnO and NiO

The *GW* approach has been applied to study the quasiparticle properties of MnO and NiO by several authors.[10,12,13,15–17,21,26] The earliest *GW* calculations for NiO were carried out with a LMTO-ASA implementation.[10] It was found that the G_0W_0@LDA corrections open the band gap from 0.2 to 1.0 eV, which is still dramatically underestimated compared to the experimental gap of ~4 eV. By further applying a nonlocal potential to e_g orbitals and updating G self-consistently, a gap of 5.5 eV was eventually obtained. Massidda *et al.* employed a self-consistent yet approximate model-*GW* scheme to study the quasiparticle band structure of MnO (Ref. 12) and NiO (Ref. 13) and obtained band gaps in good agreement with experiment. Furthermore, they observed a significant enhancement of the O 2*p* character in the highest valence-band states, in accord with the charge-transfer model of later transition-metal oxides.[117] These findings were confirmed by more recent *GW* studies.[15–17] Since many aspects of the electronic structure of MnO and NiO have already been extensively discussed in previous studies,[10,13,15–17] we will mainly focus on the effects of U in LDA+U and GW@LDA+U in this work.

Figure 4 shows the band gaps of MnO and NiO in LDA+U, G_0W_0, and GW_0 as a function of U. Unlike in ScN and ZnS, the LDA+U band gaps in MnO and NiO increase nonlinearly with increasing U, as changes in the *p*-*d* hybridization counteract the scissor behavior of $\delta\hat{V}$. The G_0W_0 and GW_0 band gaps follow accordingly and exhibit a much stronger U dependence than in ZnS and ScN or the lanthanide sesquioxides.[29] For NiO the U dependence is even more pronounced than in LDA+U, which saturates at large U. This, however, is an artifact of the LDA+U approach resulting from the fact that at around U=6 eV the *d* bands crossover with the Ni 4*s* derived states. Past this point the band gap changes little because the description of the Ni 4*s* states remains essentially at the LDA level. In GW@LDA+U, on the other hand, all bands are subject to the *GW* corrections, including Ni 4*s* derived states. Furthermore, we observe that the G_0W_0 and GW_0 corrections to the LDA+U band gap are always positive for MnO and NiO, unlike in ScN or, as we will demonstrate later, FeO. With regard to the order of G_0W_0 and GW_0 MnO behaves more like a conventional *sp* semiconductor where GW_0 gives larger band gaps than G_0W_0.[63]

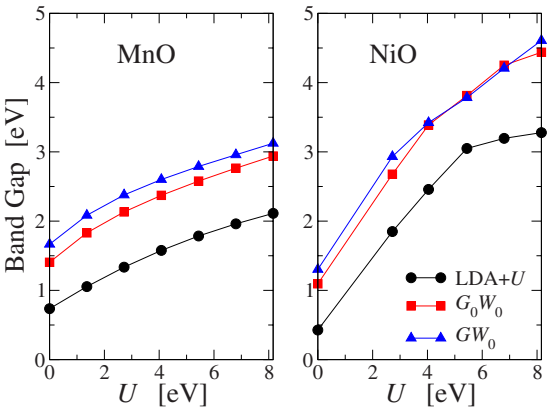

FIG. 4. (Color online) Indirect and direct band gaps of MnO and NiO in LDA+U, G_0W_0, and GW_0 as a function of U (J=0).

In Fig. 5 we illustrate the evolution of the density of states with U in LDA+U and GW_0 for MnO and NiO. Due to their similarity with GW_0 the G_0W_0 DOSs are not shown here. The most distinct feature we observe apart from the continuous band gap opening with increasing U is a narrowing of the valence bandwidth. In MnO, the LDA+U and GW_0@LDA+U valence bandwidth decreases by ~1 eV over a U range from 0 to 8.2 eV. In NiO, the LDA+U valence bandwidth first decreases and reaches a minimum at U~6 eV before it increases again, whereas GW_0@LDA +U exhibits a steady decrease by nearly 1.4 eV as U changes from 0 to 8.2 eV. In contrast to ScN and ZnS the transition-metal *d* electrons hybridize strongly with the oxygen 2*p* states and their relative energetic position determines the degree of hybridization and the width of the valence band. As the occupied 3*d* states move toward lower energy the top of the valence band develops more O 2*p* character with increasing U. This was also observed in previous *GW* calculations for MnO and NiO.[10,12,13,15,16]

To better understand the U dependence in later transition-metal oxides, we apply the same analysis to NiO that we have previously applied to ScN. Figure 6(a) shows the band

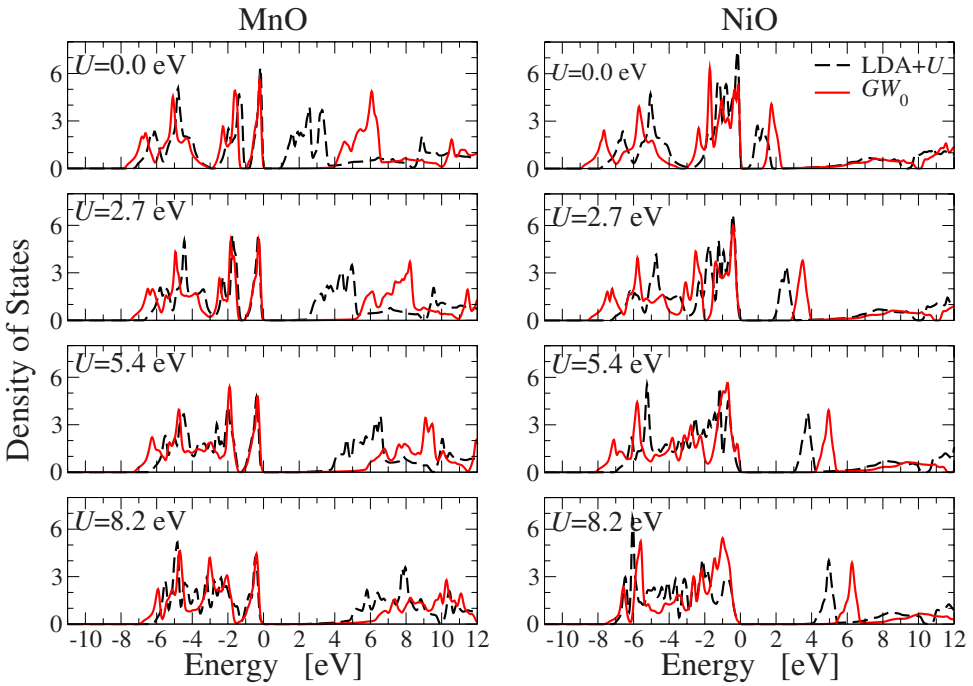

FIG. 5. (Color online) Density of states of MnO (left) and NiO (right) in LDA+U (dashed) and GW_0 (solid) for different U's; $J=0$ is used in these calculations as explained in the text.

gap at the Γ point determined with Eq. (42) and its two components as a function of U. The second term increases again as the increasing LDA+U gap decreases the screening strength. In contrast to ScN, however, the first term also grows with increasing U. This behavior can be explained by the different way that the U-correction term influences the character of the highest valence- and lowest conduction-band states. As already pointed out previously, the U correction significantly enhances the O $2p$ character in the highest valence-band states so that the latter become more delocalized as U increases. This is reflected in the quasiparticle renormalization factor $Z_{n\mathbf{k}}$, which increases significantly from 0.57 to 0.82 in the investigated U range (conventional *sp* semiconductors have renormalization factors around 0.8).[118] As a result, the first term in Eq. (42) for the valence-band maximum (VBM) state moves to lower energy as U increases. The lowest conduction-band states, on the other hand, are dominated by Ni $3d$ states at $U=0$ but become itinerant band states (of mainly Ni $4s$ character) at finite U. This is again clearly seen in the $Z_{n\mathbf{k}}$ factor, which levels out at a value of ~0.8 for U's larger than 3 eV. In that case, the term $\epsilon_{n\mathbf{k}}^{\mathrm{LDA}}$ corresponding to the conduction-band maximum state becomes constant for $U \gtrsim 3$ eV. The combination of these two factors explains why the contribution of the first term in Eq. (42) increases as a function of U. We observe that the Hubbard U correction has a much stronger influence on the hybridization between localized and itinerant states in these open d-shell transition-metal oxides than in ScN, ZnS, or the $4f$ lanthanide oxides.[29] This gives rise to a much more pronounced and nonlinear U dependence in both LDA+U

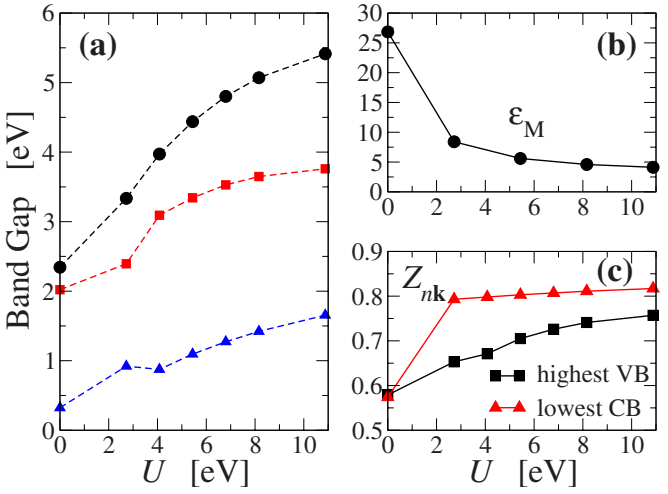

FIG. 6. (Color online) Analysis of the U dependence in NiO: (a) the direct band gap at the Γ point decomposed using Eq. (42) into contributions from the first (squares) and the second (triangles) term and their sum (circles); (b) the static macroscopic dielectric constant; and (c) the quasiparticle normalization factor $Z_{n\mathbf{k}}$.

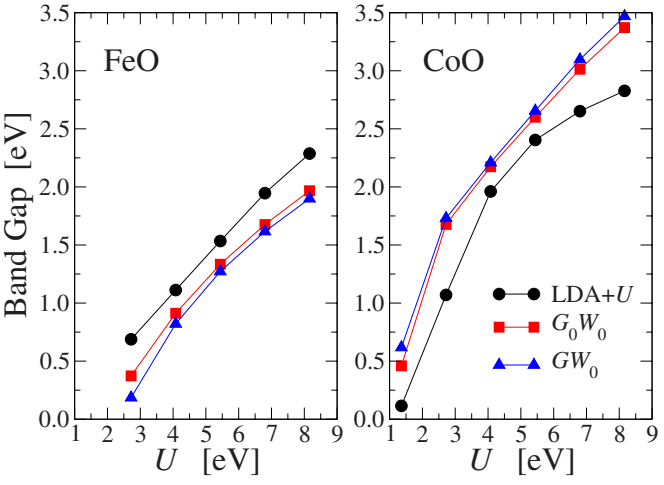

FIG. 7. (Color online) Band gap of FeO and CoO in LDA+U, G_0W_0 and GW_0 as a function of U ($J=0$).

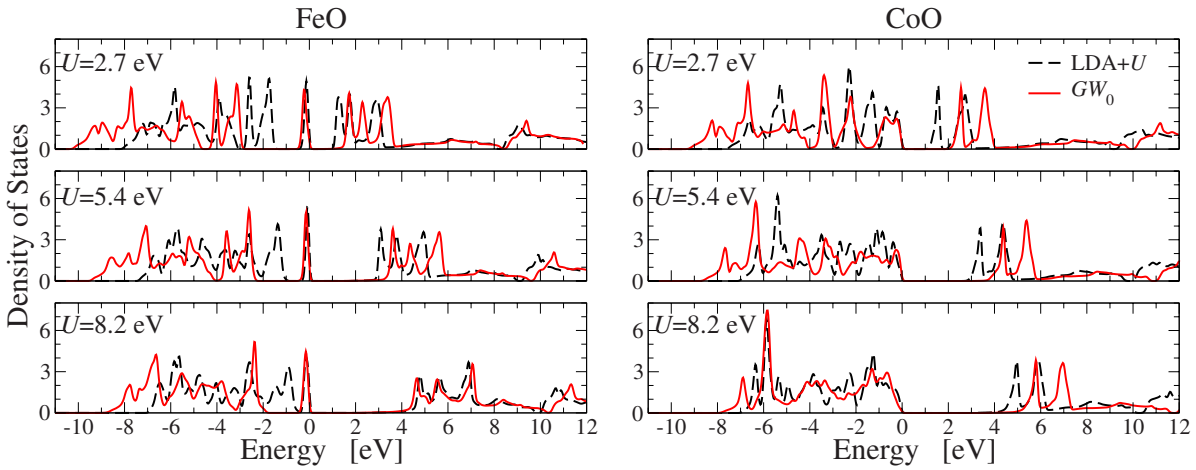

FIG. 8. (Color online) Density of states of FeO (left) and CoO (right) in LDA+U (dashed) and GW_0 (solid) for different U's (in unit of electron volt) with $J=0$.

and GW@LDA+U. This behavior is consistent with the different extent to which localized states participate in the chemical bonding in these compounds.

2. FeO and CoO

Compared to MnO and NiO, FeO and CoO are less well studied theoretically. They also pose a more serious challenge for first-principles approaches, and the first GW study for FeO and CoO has been reported only recently.[26] In a cubic crystal-field environment without symmetry breaking, the ground-state high-spin configurations of $Fe^{2+}(t_{2g}^{\uparrow 3}e_g^{\uparrow 2}t_{2g}^{\downarrow 1})$ and $Co^{2+}(t_{2g}^{\uparrow 3}e_g^{\uparrow 2}t_{2g}^{\downarrow 2})$ are degenerate, and therefore any band theory would predict FeO and CoO to be metallic. In the AFM-II phase a symmetry reduction that breaks the degeneracy is possible, but LDA and GGA, due to their strong self-interaction error, fail to induce such a break in symmetry.

Figure 7 shows the band gaps of FeO and CoO in analogy to Fig. 4. In comparison to MnO and NiO we observe several noticeable new features: (1) In FeO, the G_0W_0 and GW_0 band gaps are smaller than the LDA+U ones and in CoO the GW corrections, although similar to those in MnO and NiO, have a much smaller magnitude; (2) in both FeO and CoO, G_0W_0 and GW_0 produce nearly the same band gaps; (3) while the U dependence of the CoO band gap is similar to that of MnO and CoO, the band gap of FeO increase almost linearly as a function of U in LDA+U and to a lesser extent in G_0W_0 and GW_0.

In Fig. 8 we turn to the evolution of the DOS with U in LDA+U and GW_0. The main features, especially those of CoO, are very similar to what we have observed for MnO and NiO. The DOSs of FeO, however, show a different behavior. At small U's, the occupied states fall into four nearly separated bands. The highest band, well separated from the

TABLE III. The fundamental band gaps (in units of eV) of later transition-metal oxides from different theoretical approaches are compared to experiment.

Method	MnO	FeO	CoO	NiO
This work				
LDA+U	1.54	1.15	2.21	2.90
G_0W_0@LDA+U	2.34	0.95	2.47	3.75
GW_0@LDA+U	2.57	0.86	2.54	3.76
Other theoretical work				
G_0W_0@HSE03 (Ref. 26)	3.4	2.2	3.4	4.7
EXX-OEP (Ref. 119)	3.85	1.66	2.62	4.10
SIC-LDA (Ref. 112)	3.98	3.07	2.81	2.54
HSE03 (Ref. 26)	2.6	2.1	3.2	4.1
Experiment				
PES+BIS	3.9±0.4 (Ref. 120)		2.5±0.3 (Ref. 121)	4.3 (Ref. 122)
XAS+XES (Ref. 123)	4.1		2.6	4.0
Optical absorption	2.0 (Ref. 124)		2.7 (Ref. 125)	3.1 (Ref. 125)

other occupied states, consists of a narrow peak that is dominated by $d^{\downarrow}_{z^2}$ character. The second and third bands are very close to each other and are mainly of $(d^{\uparrow}_{xz}, d^{\uparrow}_{yz})$ and $d^{\uparrow}_{z^2}$ character, respectively, with significant admixture of other d characters and O-2p states. The last wide band is characterized by $(d^{\uparrow}_{xz}, d^{\uparrow}_{yz})$ and $(d^{\uparrow}_{x^2-y^2}, d^{\uparrow}_{xy})$ mixed with O-2p. The most noticeable feature when increasing U is that the splitting between the $d^{\downarrow}_{z^2}$ and the $(d^{\uparrow}_{xz}, d^{\uparrow}_{yz})$ bands decreases dramatically in LDA+U but changes very little in GW_0. In the fully localized limit, the LDA+U correction will shift occupied and unoccupied d bands by $\pm U/2$, respectively. Our observation of the LDA+U behavior indicates that the occupied $d^{\downarrow}_{z^2}$ band moves downward more strongly than other occupied d states. This nonuniformity of different occupied d states can be explained by the different hybridization with O 2p states: All occupied d states except $d^{\downarrow}_{z^2}$ have energetic overlap with O 2p states; as a result, the effect of the $\delta\hat{V}$ term is partially relieved by changing the hybridization strength when these states are pushed toward lower energy.

3. Comparisons with experiment

Finally we compare our GW@LDA+U results for later transition-metal oxides, using U and J determined by constrained DFT calculations, to experiment. Table III summarizes the fundamental band gaps of MnO, FeO, CoO, and NiO obtained in this work in relation to experimental and other theoretical results. Compared to widely cited experimental values, the band gaps from GW@LDA+U are considerably underestimated. We note, however, that a direct comparison of the fundamental band gap between theory and experiment has to be done with caution. An accurate experimental determination of fundamental band gaps is anything but trivial and the accuracy can be impaired by several factors, including sample quality, limited instrumental resolution, suitability of the chosen technique, or a mix of bulk and surface features. The conceptually most straightforward way to obtain band gaps is by direct and inverse PES.[126] While direct PES is now a routine technique used for probing electronic properties of occupied (including deep core and valence-band) states with ever-increasing resolution, inverse PES is not nearly as developed and the resolution is typically limited by charge accumulation on the sample surface in the course of the measurement. In practice, the band gap is therefore often measured with optical-absorption techniques. However, features in the absorption spectrum are mainly determined by dipole selection rules and the strength of the electron-hole attraction (excitonic effects).[127] In addition, the determination of the band edge can be obscured by

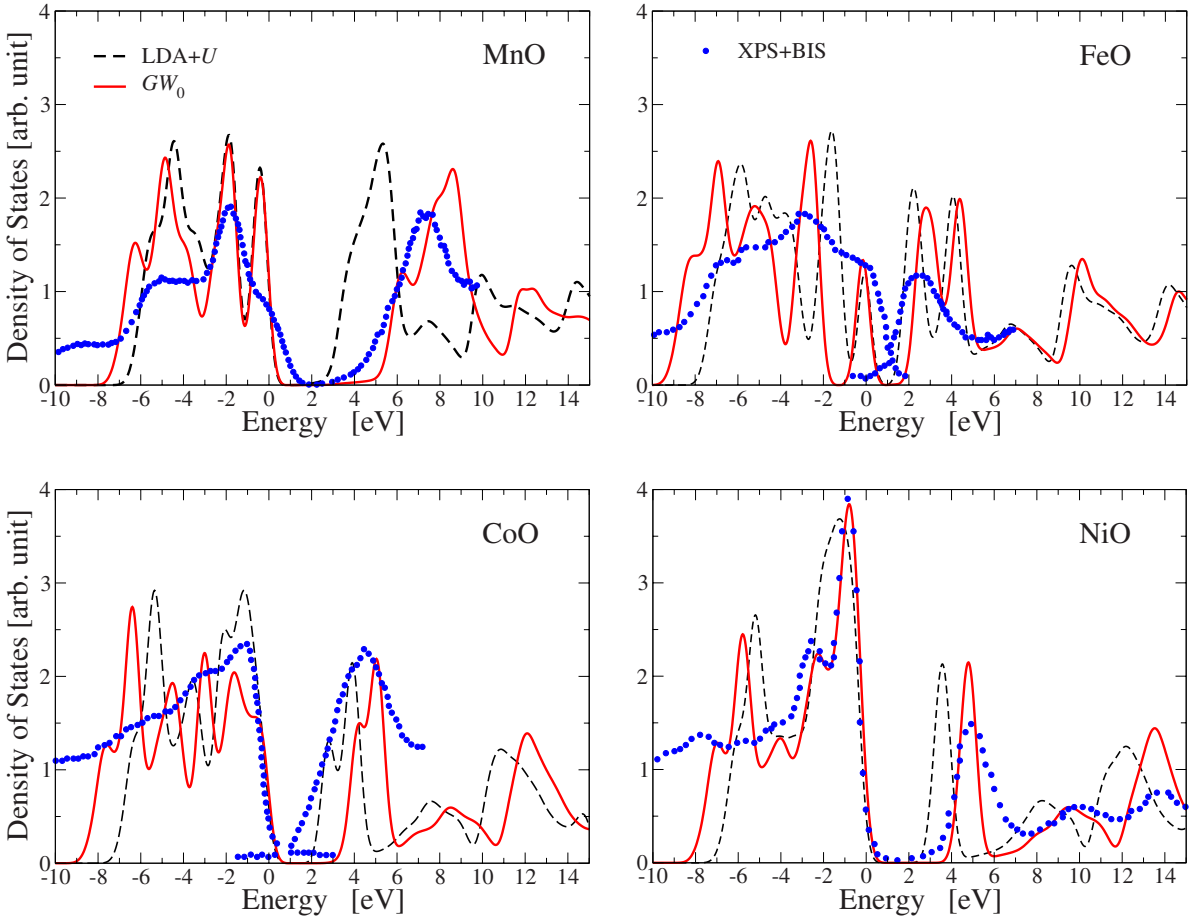

FIG. 9. (Color online) Comparison of theoretical DOS calculated by LDA+U (dashed), and GW_0 (solid) with constrained DFT U and J as listed in Table I, to experimental spectra from XPS-BIS measurements for late transition-metal monoxides. The XPS-BIS data for MnO, FeO, CoO, and NiO are extracted from Refs. 120–122 and 128, respectively.

limited resolution or the presence of impurity states. For example, different interpretations of the absorption edge of the same optical-absorption data of Powell and Spicer for NiO (Ref. 125) have given rise to widely different values for the fundamental gap (3.1, 3.5, 3.75, 4.0, and 4.3 eV).[126] Further studies in this direction and more refined experiments are clearly needed for a more unambiguous comparison between experiment and theory.

In Fig. 9, we compare the theoretical DOS with photoemission spectra [x-ray photoemission spectrum (XPS) for occupied states and bremsstrahlung-isochromat spectroscopy (BIS) for unoccupied states]. The theoretical and the experimental spectra are aligned in terms of the upper valence-band edge and/or the main VB peak position and not the Fermi level since this is not well defined at the 0 K at which the calculations are performed. Since the alignment is not unambiguous, caution has to be applied when comparing theory and experiment. In general, we observe that the DOSs from LDA+U, in spite of its great improvement over LDA, are significantly different from experiment. For GW_0@LDA+U, however, most of the peaks lie at the same position as in XPS+BIS, with the notable exception of the lowest peak in the BIS spectrum of FeO. In NiO, for example, not only the main peak in the valence-band region is accurately described but also small peaks at −2.5, −4, and −5.5 eV are all well reproduced. Difference in the peak intensities are most likely due to final-state effects in the photoemission experiments that are not taken into account in our theoretical treatment but higher order correlation effects that go beyond the GW approach cannot be ruled out at present. Another feature that is absent in the GW_0@LDA+U spectra of all four compounds is the spectral weight at higher binding energies (∼−9 eV), the so-called satellite structure. Its origin has been attributed to transitions from transition-metal d electrons[129] and it is widely believed that a many-body description beyond the GW approach is required for its description.[10,62] Our GW_0 DOSs do, however, exhibit peaks with strong d character 2 eV higher in energy. This energy difference is of the same order as the underestimation of d-electron binding energies in ZnS and other II-VI compounds and group-III nitrides and one could therefore surmise that the failure of GW has the same physical origin in both cases. This is consistent with recent observations by Shishkin *et al.*[42] that a correct description of ϵ_d in ZnS requires higher order vertex corrections in both the screened Coulomb interaction W and the self-energy.

Regarding the satellite structure in NiO, we note that the GW_0 DOSs reported in this work are obtained directly from quasiparticle energies. An alternative way to characterize electronic states of these systems is to calculate the spectral function directly from the interacting Green's function with the full energy dependence and nonhermiticity of the self-energy taken into account. The latter may well exhibit features that could be related to the satellite structure. Some analysis along this line was already conducted by Aryasetiawan and Gunnarsson (AG),[10] who concluded that the satellite structure in NiO arises from higher order correlation beyond the GW approximation. Considering the approximations employed in AG's work in which the LMTO-ASA approach was used for solving Kohn-Sham and GW equations,

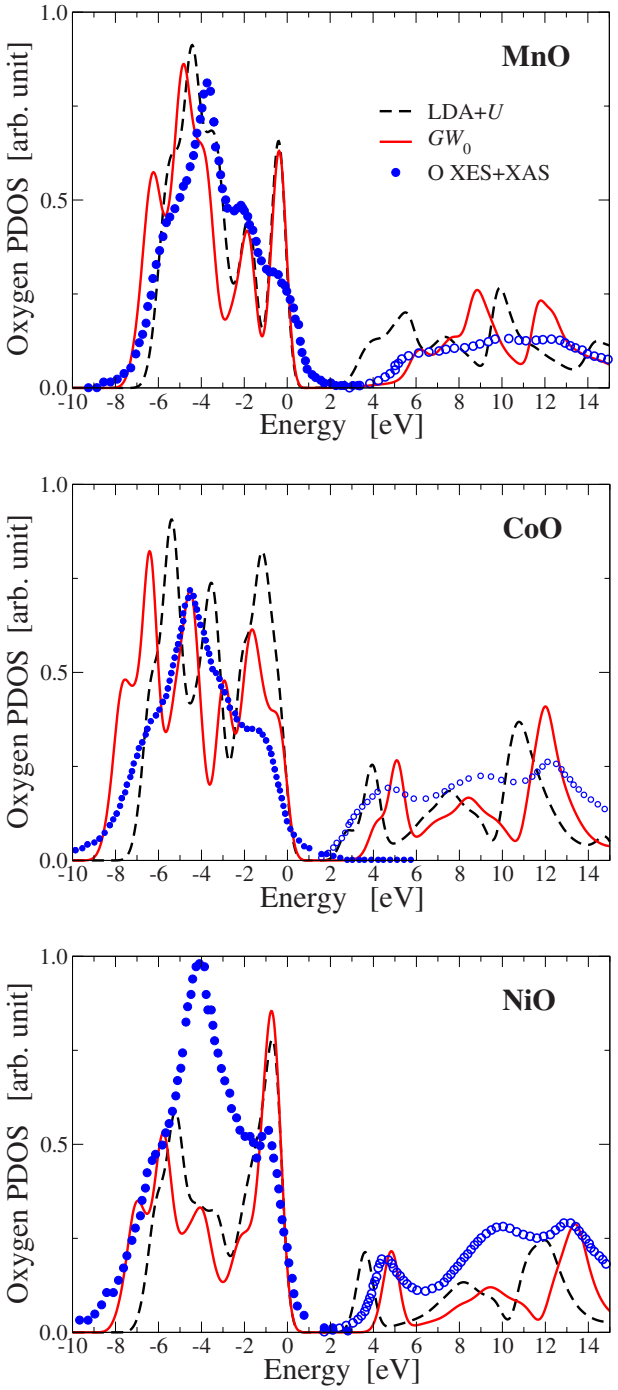

FIG. 10. (Color online) Theoretical oxygen-projected DOS in MnO, CoO, and NiO calculated by LDA+U (dashed) and GW_0@LDA+U (solid) with U and J from constrained DFT as listed in Table I are compared to oxygen x-ray emission and absorption spectra (Ref. 123).

and a nonlocal potential applied only to the e_g band was introduced to overcome the failure of LDA, we consider this issue as still not fully settled, and will pursue it in future work.

In Fig. 10 we further compare theoretical projected density of states on the oxygen atom to experimental spectra obtained from oxygen $K\alpha$ x-ray emission spectroscopy (XES) and oxygen 1s x-ray absorption spectroscopy

(XAS).[123] In our calculations we do not explicitly create a core hole, whose effect is expected to be small for oxygen emission and absorption spectra.[123,130] We also do not consider the influences of absorption cross sections. These two facts combined mean that only a comparison of peak positions and not relative intensities is meaningful. Taking this into account, we again see an overall good agreement between our *GW* results and experiment and all main features are well reproduced, in particular, the peak spacing of the three peaks in the XAS spectra of NiO.

IV. CONCLUSIONS

In this work, we employed many-body perturbation theory in the G_0W_0 and GW_0 approaches based on LDA $+U$ for a series of prototypical *d*-electron systems. We provide a derivation of the LDA$+U$ approach as an approximation to *GW*. Applied to the empty *d*-state system ScN, we found that LDA$+U$ gaps (indirect and direct) depend strongly on U, and increase linearly with U, but G_0W_0 and GW_0 band gaps exhibit only a weak U dependence. In ZnS with shallow semicore *d* states, we observe a weak band-gap dependence on U in both LDA and *GW*. *d*-electron binding energies can be tuned to their experimental value in LDA$+U$ but the *GW* corrections restore the binding energies to their value in LDA-based G_0W_0 calculations, which is considerably underestimated. In late transition-metal oxides with partially occupied *d* states, we note a strong U dependence in LDA$+U$ and GW@LDA$+U$. For U's determined from constrained DFT reasonable agreement between GW_0@LDA$+U$ and direct and inverse photoemission data is observed. The fact that the different systems show a very different U dependence in LDA$+U$ and GW@LDA$+U$ can be understood by analyzing how U changes single-particle wave functions and the screening strength in the screened Coulomb interaction W. For late transition-metal oxides the strong U dependence can then be traced back to the large U-induced change in hybridization between the oxygen $2p$ states and the transition-metal $3d$ orbitals. To be consistent the U's to be used in GW@LDA$+U$ calculations should be determined self-consistently from constrained RPA calculations[90,98,131] which will be the subject of future work. With U determined in this fashion differences between experiment and GW@LDA$+U$ would indicate where many-body effects beyond *GW* are required.

ACKNOWLEDGMENTS

This work was in part funded by the EU's Sixth Framework Programme through the NANOQUANTA (Grant No. NMP4-CT-2004-500198) network of excellence and the EU's Seventh Framework Programme through the European Theoretical Spectroscopy Facility e-Infrastructure (Grant No. 211956). Patrick Rinke acknowledges the support of the Deutsche Forschungsgemeinschaft. Hong Jiang acknowledges the support of the National Natural Science Foundation of China (Project No. 20973009).

[1] R. G. Parr and W. Yang, *Density-Functional Theory of Atoms and Molecules* (Oxford University Press, New York, 1989).
[2] R. M. Dreizler and E. K. U. Gross, *Density Functional Theory: An Approach to the Quantum Many-Body Problem* (Springer-Verlag, Berlin, 1990).
[3] R. M. Martin, *Electronic Structure* (Cambridge University Press, Cambridge, UK, 2004).
[4] J. C. Slater, *Quantum Theory of Molecules and Solids* (McGraw-Hill, New York, 1974), Vol. 4.
[5] J. F. Janak, Phys. Rev. B **18**, 7165 (1978).
[6] F. Aryasetiawan and O. Gunnarsson, Rep. Prog. Phys. **61**, 237 (1998).
[7] K. Terakura, T. Oguchi, A. R. Williams, and J. Kübler, Phys. Rev. B **30**, 4734 (1984).
[8] L. Hedin, Phys. Rev. **139**, A796 (1965).
[9] F. Aryasetiawan, Phys. Rev. B **46**, 13051 (1992).
[10] F. Aryasetiawan and O. Gunnarsson, Phys. Rev. Lett. **74**, 3221 (1995).
[11] F. Aryasetiawan and K. Karlsson, Phys. Rev. B **54**, 5353 (1996).
[12] S. Massidda, A. Continenza, M. Posternak, and A. Baldereschi, Phys. Rev. Lett. **74**, 2323 (1995).
[13] S. Massidda, A. Continenza, M. Posternak, and A. Baldereschi, Phys. Rev. B **55**, 13494 (1997).
[14] A. Yamasaki and T. Fujiwara, Phys. Rev. B **66**, 245108 (2002).
[15] S. V. Faleev, M. van Schilfgaarde, and T. Kotani, Phys. Rev. Lett. **93**, 126406 (2004).
[16] J.-L. Li, G.-M. Rignanese, and S. G. Louie, Phys. Rev. B **71**, 193102 (2005).
[17] C. H. Patterson, Int. J. Quantum Chem. **106**, 3383 (2006).
[18] F. Bruneval, N. Vast, L. Reining, M. Izquierdo, F. Sirotti, and N. Barrett, Phys. Rev. Lett. **97**, 267601 (2006).
[19] A. N. Chantis, M. van Schilfgaarde, and T. Kotani, Phys. Rev. B **76**, 165126 (2007).
[20] M. Gatti, F. Bruneval, V. Olevano, and L. Reining, Phys. Rev. Lett. **99**, 266402 (2007).
[21] C. Rödl, F. Fuchs, J. Furthmüller, and F. Bechstedt, Phys. Rev. B **77**, 184408 (2008).
[22] T. Kotani, M. van Schilfgaarde, and S. V. Faleev, Phys. Rev. B **76**, 165106 (2007).
[23] A. N. Chantis, R. C. Albers, M. D. Jones, M. van Schilfgaarde, and T. Kotani, Phys. Rev. B **78**, 081101(R) (2008).
[24] R. Sakuma, T. Miyake, and F. Aryasetiawan, Phys. Rev. B **78**, 075106 (2008).
[25] S. Kobayashi, Y. Nohara, S. Yamamoto, and T. Fujiwara, Phys. Rev. B **78**, 155112 (2008).
[26] C. Rödl, F. Fuchs, J. Furthmüller, and F. Bechstedt, Phys. Rev. B **79**, 235114 (2009).
[27] Y. Nohara, S. Yamamoto, and T. Fujiwara, Phys. Rev. B **79**, 195110 (2009).
[28] R. Sakuma, T. Miyake, and F. Aryasetiawan, Phys. Rev. B **80**, 235128 (2009).
[29] H. Jiang, R. I. Gomez-Abal, P. Rinke, and M. Scheffler, Phys.

Rev. Lett. **102**, 126403 (2009).
[30] H. Jiang, Acta. Phys. -Chim. Sin. **26**, 1017 (2010).
[31] M. Rohlfing, P. Krüger, and J. Pollmann, Phys. Rev. Lett. **75**, 3489 (1995).
[32] P. Rinke, A. Qteish, J. Neugebauer, C. Freysoldt, and M. Scheffler, New J. Phys. **7**, 126 (2005).
[33] W. Nelson, P. Bokes, P. Rinke, and R. W. Godby, Phys. Rev. A **75**, 032505 (2007).
[34] F. Fuchs, J. Furthmüller, F. Bechstedt, M. Shishkin, and G. Kresse, Phys. Rev. B **76**, 115109 (2007).
[35] P. Rinke, A. Qteish, J. Neugebauer, and M. Scheffler, Phys. Status Solidi B **245**, 929 (2008).
[36] S. Biermann, F. Aryasetiawan, and A. Georges, Phys. Rev. Lett. **90**, 086402 (2003).
[37] P. Sun and G. Kotliar, Phys. Rev. Lett. **92**, 196402 (2004).
[38] A. Schindlmayr and R. W. Godby, Phys. Rev. Lett. **80**, 1702 (1998).
[39] A. J. Morris, M. Stankovski, K. Delaney, P. Rinke, P. García-González, and R. W. Godby, Phys. Rev. B **76**, 155106 (2007).
[40] M. van Schilfgaarde, T. Kotani, and S. V. Faleev, Phys. Rev. B **74**, 245125 (2006).
[41] F. Bruneval, N. Vast, and L. Reining, Phys. Rev. B **74**, 045102 (2006).
[42] M. Shishkin, M. Marsman, and G. Kresse, Phys. Rev. Lett. **99**, 246403 (2007).
[43] V. I. Anisimov, J. Zaanen, and O. K. Andersen, Phys. Rev. B **44**, 943 (1991).
[44] V. I. Anisimov, I. V. Solovyev, M. A. Korotin, M. T. Czyzyk, and G. A. Sawatzky, Phys. Rev. B **48**, 16929 (1993).
[45] A. I. Liechtenstein, V. I. Anisimov, and J. Zaanen, Phys. Rev. B **52**, R5467 (1995).
[46] V. I. Anisimov, F. Aryasetiawan, and A. I. Lichtenstein, J. Phys.: Condens. Matter **9**, 767 (1997).
[47] T. Miyake, P. Zhang, M. L. Cohen, and S. G. Louie, Phys. Rev. B **74**, 245213 (2006).
[48] H. J. de Groot, P. A. Bobbert, and W. van Haeringen, Phys. Rev. B **52**, 11000 (1995).
[49] U. von Barth and B. Holm, Phys. Rev. B **54**, 8411 (1996).
[50] E. L. Shirley, Phys. Rev. B **54**, 7758 (1996).
[51] B. Holm and U. von Barth, Phys. Rev. B **57**, 2108 (1998).
[52] W.-D. Schöne and A. G. Eguiluz, Phys. Rev. Lett. **81**, 1662 (1998).
[53] W. Ku and A. G. Eguiluz, Phys. Rev. Lett. **89**, 126401 (2002).
[54] K. Delaney, P. Garcia-Gonzalez, A. Rubio, P. Rinke, and R. W. Godby, Phys. Rev. Lett. **93**, 249701 (2004).
[55] A. Stan, N. E. Dahlen, and R. van Leeuwen, Europhys. Lett. **76**, 298 (2006).
[56] A. Stan, N. E. Dahlen, and R. van Leeuwen, J. Chem. Phys. **130**, 114105 (2009).
[57] A. Kutepov, S. Y. Savrasov, and G. Kotliar, Phys. Rev. B **80**, 041103(R) (2009).
[58] K. Kaasbjerg and K. S. Thygesen, Phys. Rev. B **81**, 085102 (2010).
[59] C. Rostgaard, K. W. Jacobsen, and K. S. Thygesen, Phys. Rev. B **81**, 085103 (2010).
[60] A. Schindlmayr, Phys. Rev. B **56**, 3528 (1997).
[61] A. Schindlmayr, P. Garcia-Gonzalez, and R. W. Godby, Phys. Rev. B **64**, 235106 (2001).
[62] F. Aryasetiawan, in *Strong Coulomb Correlations in Electronic Structure Calculations: Beyond the Local Density Approximation*, edited by V. I. Anisimov (Gordon and Breach Science, Singapore, 2000), p. 1.
[63] M. Shishkin and G. Kresse, Phys. Rev. B **75**, 235102 (2007).
[64] M. van Schilfgaarde, T. Kotani, and S. Faleev, Phys. Rev. Lett. **96**, 226402 (2006).
[65] F. Bechstedt, F. Fuchs, and G. Kresse, Phys. Status Solidi B **246**, 1877 (2009).
[66] W. G. Aulbur, M. Städele, and A. Görling, Phys. Rev. B **62**, 7121 (2000).
[67] V. I. Anisimov and O. Gunnarsson, Phys. Rev. B **43**, 7570 (1991).
[68] I. Lindgren and J. Morrison, *Atomic Many-Body Theory*, Springer Series in Chemical Physics Vol. 13 (Springer-Verlag, Berlin, 1982).
[69] F. M. F. de Groot, J. C. Fuggle, B. T. Thole, and G. A. Sawatzky, Phys. Rev. B **42**, 5459 (1990).
[70] M. T. Czyżyk and G. A. Sawatzky, Phys. Rev. B **49**, 14211 (1994).
[71] S. L. Dudarev, G. A. Botton, S. Y. Savrasov, C. J. Humphreys, and A. P. Sutton, Phys. Rev. B **57**, 1505 (1998).
[72] A. G. Petukhov, I. I. Mazin, L. Chioncel, and A. I. Lichtenstein, Phys. Rev. B **67**, 153106 (2003).
[73] E. R. Ylvisaker, W. E. Pickett, and K. Koepernik, Phys. Rev. B **79**, 035103 (2009).
[74] I. V. Solovyev, P. H. Dederichs, and V. I. Anisimov, Phys. Rev. B **50**, 16861 (1994).
[75] P. Blaha, K. Schwarz, G. K. H. Madsen, D. Kvasnicka, and J. Luitz, *WIEN2k, An Augmented Plane Wave + Local Orbitals Program for Calculating Crystal Properties*, edited by K. Schwarz (Techn. Universität Wien, Austria, 2001).
[76] K. Schwarz, P. Blaha, and G. K. H. Madsen, Comput. Phys. Commun. **147**, 71 (2002).
[77] P. Novák, F. Boucher, P. Gressier, P. Blaha, and K. Schwarz, Phys. Rev. B **63**, 235114 (2001).
[78] R. Gómez-Abal, X. Li, M. Scheffler, and C. Ambrosch-Draxl, Phys. Rev. Lett. **101**, 106404 (2008).
[79] R. Gomez-Abal, X. Li, H. Jiang, and M. Scheffler (unpublished).
[80] H. Jiang, R. I. Gomez-Abal, P. Rinke, and M. Scheffler, Phys. Rev. B **81**, 085119 (2010).
[81] W. E. Pickett, H. Krakauer, and P. B. Allen, Phys. Rev. B **38**, 2721 (1988).
[82] D. Gall, I. Petrov, N. Hellgren, L. Hultman, J. E. Sundgren, and J. E. Greene, J. Appl. Phys. **84**, 6034 (1998).
[83] F. Tran, P. Blaha, K. Schwarz, and P. Novak, Phys. Rev. B **74**, 155108 (2006).
[84] W. E. Pickett, S. C. Erwin, and E. C. Ethridge, Phys. Rev. B **58**, 1201 (1998).
[85] M. Cococcioni and S. de Gironcoli, Phys. Rev. B **71**, 035105 (2005).
[86] P. H. Dederichs, S. Blügel, R. Zeller, and H. Akai, Phys. Rev. Lett. **53**, 2512 (1984).
[87] M. Springer and F. Aryasetiawan, Phys. Rev. B **57**, 4364 (1998).
[88] T. Kotani, J. Phys.: Condens. Matter **12**, 2413 (2000).
[89] F. Aryasetiawan, M. Imada, A. Georges, G. Kotliar, S. Biermann, and A. I. Lichtenstein, Phys. Rev. B **70**, 195104 (2004).
[90] F. Aryasetiawan, K. Karlsson, O. Jepsen, and U. Schönberger, Phys. Rev. B **74**, 125106 (2006).
[91] K. Nakamura, R. Arita, Y. Yoshimoto, and S. Tsuneyuki, Phys. Rev. B **74**, 235113 (2006).
[92] N. J. Mosey, P. Liao, and E. A. Carter, J. Chem. Phys. **129**,

014103 (2008).
[93] A. K. McMahan, R. M. Martin, and S. Satpathy, Phys. Rev. B **38**, 6650 (1988).
[94] M. S. Hybertsen, M. Schlüter, and N. E. Christensen, Phys. Rev. B **39**, 9028 (1989).
[95] G. K. H. Madsen and P. Novak, Europhys. Lett. **69**, 777 (2005).
[96] Pan Wei and Z. Q. Qi, Phys. Rev. B **49**, 10864 (1994).
[97] O. Bengone, M. Alouani, P. Blöchl, and J. Hugel, Phys. Rev. B **62**, 16392 (2000).
[98] T. Miyake and F. Aryasetiawan, Phys. Rev. B **77**, 085122 (2008).
[99] C. Stampfl, W. Mannstadt, R. Asahi, and A. J. Freeman, Phys. Rev. B **63**, 155106 (2001).
[100] A. Qteish, P. Rinke, M. Scheffler, and J. Neugebauer, Phys. Rev. B **74**, 245208 (2006).
[101] D. Gall, M. Städele, K. Järrendahl, I. Petrov, P. Desjardins, R. T. Haasch, T. Y. Lee, and J. E. Greene, Phys. Rev. B **63**, 125119 (2001).
[102] H. A. Al-Brithen and A. R. Smith, Appl. Phys. Lett. **77**, 2485 (2000).
[103] H. A. Al-Brithen, A. R. Smith, and D. Gall, Phys. Rev. B **70**, 045303 (2004).
[104] T.-Y. Lü and M.-C. Huang, Chin. Phys. **16**, 62 (2007).
[105] O. Zakharov, A. Rubio, X. Blase, M. L. Cohen, and S. G. Louie, Phys. Rev. B **50**, 10780 (1994).
[106] F. Aryasetiawan and O. Gunnarsson, Phys. Rev. B **54**, 17564 (1996).
[107] M. Rohlfing, P. Krüger, and J. Pollmann, Phys. Rev. B **57**, 6485 (1998).
[108] W. Luo, S. Ismail-Beigi, M. L. Cohen, and S. G. Louie, Phys. Rev. B **66**, 195215 (2002).
[109] A. Fleszar and W. Hanke, Phys. Rev. B **71**, 045207 (2005).
[110] P. Rinke, M. Winkelnkemper, A. Qteish, D. Bimberg, J. Neugebauer, and M. Scheffler, Phys. Rev. B **77**, 075202 (2008).
[111] A. Janotti, D. Segev, and C. G. Van de Walle, Phys. Rev. B **74**, 045202 (2006).
[112] A. Svane and O. Gunnarsson, Phys. Rev. Lett. **65**, 1148 (1990).
[113] J. Hugel and M. Kamal, Solid State Commun. **100**, 457 (1996).
[114] X. Ren, I. Leonov, G. Keller, M. Kollar, I. Nekrasov, and D. Vollhardt, Phys. Rev. B **74**, 195114 (2006).
[115] J. Kuneš, V. I. Anisimov, S. L. Skornyakov, A. V. Lukoyanov, and D. Vollhardt, Phys. Rev. Lett. **99**, 156404 (2007).
[116] S. Sharma, J. K. Dewhurst, N. N. Lathiotakis, and E. K. U. Gross, Phys. Rev. B **78**, 201103(R) (2008).
[117] J. Zaanen, G. A. Sawatzky, and J. W. Allen, Phys. Rev. Lett. **55**, 418 (1985).
[118] The increase in the band gap can also lead to increasing Z since the peak structure in W arising from the gap states is shifted toward higher energy, resulting in less steep $\Re\Sigma(\epsilon)$. However, the increase in Z in NiO is largely related to the enhanced O $2p$ character at the VBM. This is consistent with the fact that for other systems, e.g., ScN, the change in Z as a function of U is very small (Z changes from 0.73 to 0.74 when U increases from 2.0 to 8.2 eV).
[119] E. Engel and R. N. Schmid, Phys. Rev. Lett. **103**, 036404 (2009).
[120] J. van Elp, R. H. Potze, H. Eskes, R. Berger, and G. A. Sawatzky, Phys. Rev. B **44**, 1530 (1991).
[121] J. van Elp, J. L. Wieland, H. Eskes, P. Kuiper, G. A. Sawatzky, F. M. F. de Groot, and T. S. Turner, Phys. Rev. B **44**, 6090 (1991).
[122] G. A. Sawatzky and J. W. Allen, Phys. Rev. Lett. **53**, 2339 (1984).
[123] E. Z. Kurmaev, R. G. Wilks, A. Moewes, L. D. Finkelstein, S. N. Shamin, and J. Kunes, Phys. Rev. B **77**, 165127 (2008).
[124] D. R. Huffman, R. L. Wild, and M. Shinmei, J. Chem. Phys. **50**, 4092 (1969).
[125] R. J. Powell and W. E. Spicer, Phys. Rev. B **2**, 2182 (1970).
[126] S. Hüfner, *Photoelectron Spectroscopy: Principles and Applications*, 3rd ed. (Springer, Berlin, 2003).
[127] P. Y. Yu and M. Cardona, *Fundamentals of Semiconductors: Physics and Materials Properties*, 3rd ed. (Springer, Berlin, 2001).
[128] R. Zimmermann, P. Steiner, R. Claessen, F. Reinert, S. Hüfner, P. Blaha, and P. Dufek, J. Phys.: Condens. Matter **11**, 1657 (1999).
[129] S. Hüfner, Adv. Phys. **43**, 183 (1994).
[130] L. V. Dobysheva, P. L. Potapov, and D. Schryvers, Phys. Rev. B **69**, 184404 (2004).
[131] T. Miyake, F. Aryasetiawan, and M. Imada, Phys. Rev. B **80**, 155134 (2009).